fMRI predictors based on language models of increasing complexity recover brain left lateralization

Laurent Bonnasse-Gahot
Centre d'Analyse et de Mathématique Sociales
CNRS, EHESS
75006 Paris, France
lbg@ehess.fr

Christophe Pallier
Cognitive Neuroimaging Unit
CNRS, INSERM, CEA, Neurospin center
91191 Gif-sur-Yvette, France
christophe@pallier.org

Abstract

Over the past decade, studies of naturalistic language processing where participants are scanned while listening to continuous text have flourished. Using word embeddings at first, then large language models, researchers have created encoding models to analyze the brain signals. Presenting these models with the same text as the participants allows to identify brain areas where there is a significant correlation between the functional magnetic resonance imaging (fMRI) time series and the ones predicted by the models' artificial neurons. One intriguing finding from these studies is that they have revealed highly symmetric bilateral activation patterns, somewhat at odds with the well-known left lateralization of language processing. Here, we report analyses of an fMRI dataset where we manipulate the complexity of large language models, testing 28 pretrained models from 8 different families, ranging from 124M to 14.2B parameters. First, we observe that the performance of models in predicting brain responses follows a scaling law, where the fit with brain activity increases linearly with the logarithm of the number of parameters of the model (and its performance on natural language processing tasks). Second, although this effect is present in both hemispheres, it is stronger in the left than in the right hemisphere. Specifically, the left-right difference in brain correlation follows a scaling law with the number of parameters. This finding reconciles computational analyses of brain activity using large language models with the classic observation from aphasic patients showing left hemisphere dominance for language.

1 Introduction

Since the seminal discovery that language disorders are most often associated with lesions to the brain's left hemisphere (Dax, 1865; Manning and Thomas-Antérion, 2011; Broca, 1865; Wernicke, 1874), the existence of a left-right asymmetry in the cortical processing of language has been amply documented through different approaches, e.g., studies of split-brain patients (Gazzaniga and Sperry, 1967), intracarotid amobarbital injections (Wada and Rasmussen, 1960), electrocortical stimulation (Penfield and Roberts, 1959), functional brain imaging (Binder et al., 1996; Just et al., 1996; Stromswold et al., 1996; Malik-Moraleda et al., 2022), and behavioral measurements such as reaction times to words presented in the left or right visual fields (Hausmann et al., 2019). All in all, even if there is clear evidence that the right hemisphere is implicated in speech and language processing (Bookheimer, 2002; Jung-Beeman, 2005; Lerner et al., 2011; Vigneau et al., 2011; Bradshaw et al., 2017), it is estimated that left hemispheric dominance for language occurs in approximately 90% of healthy individuals (Josse and Tzourio-Mazoyer, 2004; Tzourio-Mazoyer et al., 2017).

38th Conference on Neural Information Processing Systems (NeurIPS 2024).

Given this state of affairs, one can only be surprised by the symmetric patterns highlighted by studies that have relied on computational models of language to predict fMRI brain time-courses in participants listening to naturalistic texts (e.g. Huth et al., 2016; Heer et al., 2017; Toneva and Wehbe, 2019; Caucheteux et al., 2021; Schrimpf et al., 2021; Pasquiou et al., 2023). For example, Huth et al. (2016) constructed word embeddings using a latent-semantic approach based on co-occurrence counts (Landauer and Dumais, 1997) and used them as predictors of brain activity while participants listened to stories. The maps revealed by this approach were strikingly symmetric. This finding was replicated in subsequent studies that have used predictors derived from more advanced language models based on LSTM (Jain and Huth, 2018) or Transformers (e.g. Toneva and Wehbe, 2019; Caucheteux et al., 2021; Schrimpf et al., 2021; Pasquiou et al., 2023) (but see Caucheteux and King, 2022 who reported a significant left-right asymmetry). One potential interpretation is that brain scores are essentially driven by semantic representations (Kauf et al., 2024), supposedly represented in a very distributed fashion across both hemispheres (see e.g. the discussion in Huth et al., 2016).

In this paper, we use 28 large language models (LLMs) of increasing size (from GPT-2 with 124 million parameters to Qwen1.5-14B with 14.2 billion parameters; see Table A.1 for the full list) to fit fMRI data obtained from participants who listened to a naturalistic text (from *Le Petit Prince* dataset, Li et al., 2022). We find that a clear left-right asymmetry emerges as the size and performance of these models increases, and that this is not simply due to differences in signal-to-noise ratio between left and right hemispheres.

2 Methods

2.1 fMRI data

***Le Petit Prince* dataset.** We use the publicly available fMRI dataset *Le Petit Prince*[1] which provides recordings from English, French and Chinese participants who had listened to the audiobook of *Le Petit Prince* in their native language while being scanned using functional magnetic resonance (TR=2 s; voxel size=3.75 × 3.75 × 3.8 mm). Technical details on fMRI acquisition and preprocessing can be found in the publication accompanying the dataset (Li et al., 2022). Here, we use fMRI data spatially normalized in the Montreal Neurological Institute space, from all 49 English speakers. All of them were right-handed according to the Edinburgh handedness questionnaire. For each participant, fMRI acquisition was divided into 9 runs lasting each for about 10 min.

Additional preprocessing and creation of an average subject. To reduce the computational burden of the study, and because we are interested in making inferences about the general population, we compute a group average from all subjects. In order to further reduce the computational cost of the study, all functional data are first resampled to 4 mm isotropic voxels, close to the original acquisition resolution. Before averaging, we compute a symmetric brain mask common to all subjects using `nilearn` `compute_multi_epi_mask` function with the threshold parameter set at 50%. The resulting mask, henceforth named *whole brain volume*, comprises 25870 voxels (1656 cm^3). For all subjects and each run independently, voxels' time-series are high-pass filtered with a cut-off of 128 s, linearly detrended and standardized (zero mean and unit variance). We then compute the average subject by taking the mean of all these values per voxel and per run. Finally, we trim the first 20 s and the last 20 s of each run, as these were found to present deviation artifacts, and standardize the resulting time-series.

Inter-subjects reliable voxels. In order to evaluate the signal-to-noise ratio in each voxel, independently of any language model, we estimate the reliability of each voxel across participants. To do so, we split the group of all 49 subjects into two (almost) equal subgroups (24/25), compute the average response for each group and predict the BOLD time series from each voxel of one group from the activity of all the voxels from the other group. The fitting procedure follows the same method described in more details below when fitting brain response with neural network activations, and is based on a linear mapping from one set of responses to another, evaluated on a held-out run through cross-validation, and regularized using ridge regression (L2). For each run, for each voxel, we thus compute the correlation between the true activity and the activity predicted from the other group of subjects, with a linear model trained on the other runs. This procedure is repeated 10 times, using

[1] `https://openneuro.org/datasets/ds003643/versions/2.0.5`

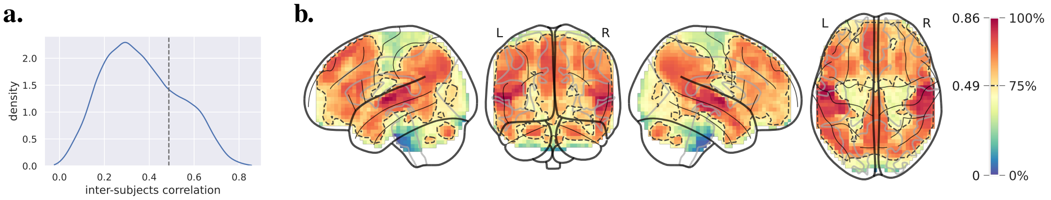

Figure 1: **Inter-subjects reliable voxels**. (a) Distribution of inter-subjects correlations over voxels, computed using two subgroups of subjects and predicting one subgroup average fMRI time-course from the other one (see main text for details). Voxels with a brain correlation above the dotted vertical line represent the 25% voxels with the largest correlations. (b) Glass brain representation of this inter-subjects reliability measure. Hot colors and dotted line show the 25% most reliable voxels.

different splits of the subjects. The final inter-group correlation for each voxel is the average over these 10 trials, and is plotted in Fig. 1. The resulting map is quite consistent to the ones obtained in previous inter-subjects correlations language studies (e.g. Lerner et al., 2011). The plots presented in the main paper are based on the subset of the 25% most reliable voxels, representing a total of 6468 voxels (414 cm^3) – 3297 in the left hemisphere and 3171 in the right hemisphere. These voxels are in hot-colored regions delineated with the dashed lines on Fig. 1. In Fig. B.1, inter-subjects correlations averaged over parcels defined by the Harvard-Oxford atlas are plotted. The graphics in panels (b) and (c) reveal a strong relationship between correlations in the left and right homologous regions, with a tendency toward stronger correlations in the left than in the homologous right regions.

Regions of Interest. We selected a set of a priori regions of interest from previous works on syntactic and semantic composition: the Temporal Pole (TP), anterior Superior Temporal Sulcus (aSTS) and posterior Superior Temporal Sulcus (pSTS) from Pallier et al. (2011), the Inferior Frontal Gyrus pars opercularis (BA44), triangularis (BA44) and orbitalis (BA47) from Zaccarella et al. (2017), and the Angular Gyrus/Temporal Parietal Junction (AG/TPJ) from Price et al. (2015). Each region was defined as a sphere of 10 mm radius centered on the following coordinates in the Montreal Neurological Institute's MNI152 space : TP (-48, 15, -27), aSTS (-54, -12, -12), pSTS (-51, -39, 3), AG/TPJ (-52, -56, 22), BA44 (-50, 12, 16), BA45 (-52, 28, 10), BA47 (-44,34,-8).

2.2 Encoding models

Language models. We used 28 pretrained models, all available on the Hugging Face hub, ranging from 124M to 14.2B parameters. The full list along with some details on the number of parameters, layers and hidden size (number of neurons n_{neurons} at the output of each layer) is provided in Table A.1 on page 16 in Appendix. These pretrained models come from 8 different families, namely GPT-2 (Radford et al., 2019), OPT (Zhang et al., 2022), Llama 2 (Touvron et al., 2023), Qwen (Bai et al., 2023), gemma (Team et al., 2024), Stable LM (Bellagente et al., 2024), Mistral (Jiang et al., 2023), and Mamba (Gu and Dao, 2023). In this study, we only consider base models, trained with the same next-word prediction task. Most models are based on the Transformer decoder architecture (Vaswani et al., 2017), apart from the Mamba family, which is a recent come-back of the recurrent neural network approach that is competitive with the Transformer language models.
In order to extract the activation of each model in response to the text of *The Little Prince*, each model is fed with the full original English text. We make use of the time-aligned speech segmentation provided in the *Le Petit Prince* openneuro.org repository, to align the activity of the neural networks with what the subjects heard in the scanner. Each word in the text is associated with its onset in the audiobook, and the representation that we compute is the average of all the vectors of all the tokens that constitute this word, as well as the following punctuation marks if there are any. Finally, in order to mimic the BOLD response, the activity of the artificial neural network under consideration is convolved with the Glover haemodynamic response function (Glover, 1999), as implemented in the `nilearn` package.

Baseline models. In addition to considering all these pretrained language models, we look at a few baselines to compare with. First, we consider purely random vectors, aligned with the word onsets. Second, we consider random embeddings, similar to the previous case, but where each word is always associated with the same (random) vector. In these two cases, we look at 300 and 1024 dimensional vectors. The results presented in this paper for these random baselines were averaged over 10 models obtained from different seeds. Third, we look at non-contextual embeddings provided by the seminal GloVe embeddings, where each word is always associated with the same vector, of 300 dimensions here, after training on co-occurrences on large English text corpora (Pennington et al., 2014).

Procedure for fitting an encoding model. For each model, we separately consider the activity provided by each layer, plus the embedding layer. Hence, for a 12-layer model, we consider 13 layers. Let us notate $X_{l,k}$ the activity of a layer l generated by the text of run k, (after convolution with the haemodynamic response function, as described above), and $Y_{v,k}$ the BOLD time series of voxel v of run k. $X_{l,k}$ is a $n_{\text{scans},k} \times n_{\text{neurons}}$ matrix, and $Y_{v,k}$ a vector of dimension $n_{\text{scans},k}$, where $n_{\text{scans},k}$ is the number of scans of run k, and n_{neurons} the number of dimensions of layer l (for instance, gpt2-large model has 1280 dimensions, and Mistral-7B-v0.1 has 4096 dimensions). The goal is to predict the functional brain activity $Y_{v,k}$ using the artificial neural activity $X_{l,k}$ as regressors, simply using a linear mapping between the two: $\widehat{Y_{v,k}} = X_{l,k}\beta$, where β is a vector of dimension n_{neurons}. In order to avoid overfitting, the β coefficients are determined using ridge regression with regularization strength controlled by the parameter α. More precisely, given a run k used as test, all the remaining 8 runs are used as training set to determine the β coefficients. The hyperparameter α is chosen using nested cross-validation among a range of possible values (16 values log-spaced between 10^2 and 10^7): among the runs used for training, one is used for validation, and the remaining 7 runs for training the ridge regression with each value of α. Correlation between the actual values $Y_{v,\text{val}}$ and the predicted ones $\widehat{Y_{v,\text{val}}}$ is used to decide which value of α is used during training: the best α is chosen as the one yielding the greatest correlation averaged over all voxels [2]. This value is then used to compute the ridge regression on the training runs and predict the functional brain activity on the test run k. The brain correlation for a given voxel v and a given layer l is given by repeating this procedure for all 9 runs and taking the average correlation: $1/n_{\text{runs}} \sum_{k=1}^{n_{\text{runs}}} \text{corr}(Y_{v,k}; \widehat{Y_{v,k}})$. In the end, for a given voxel, we take as brain correlation the best correlation when considering all the layers of the model.

2.3 Computer code

The Python 3.10 code written for the present project relies on the following libraries: `transformers v4.40.1` (Wolf et al., 2020), `scikit_learn v1.4.2` (Pedregosa et al., 2011), `nilearn v0.10.4`, `Pytorch v2.3.0` (Paszke et al., 2019), `matplotlib v3.8.4` (Hunter, 2007), `seaborn v0.13.2` (Waskom, 2021), `numpy v1.26.4` (Van Der Walt et al., 2011), `pandas v2.2.2` (McKinney et al., 2010), `statsmodels v0.14.2` (Seabold and Perktold, 2010). All pretrained models were downloaded from Hugging Face through the `transformers` interface. The code is available at `https://github.com/l-bg/llms_brain_lateralization`.

The main English study on the average subject takes about five days of CPU time on a computer equipped with an Intel Xeon w5-3425 processor (12 cores), mainly dedicated to perform the ridge regression of all layers of all models, using the `scikit-learn` package.

3 Results

3.1 Distribution of correlations

The distributions of correlations over voxels, for each model, are displayed on panel (a) of Fig. 2 for the 25% most reliable voxels, and of Fig. B.2 for the whole brain volume. The random vector baseline yields very low brain correlations centered around 0. Random embeddings (fixed random vector for each word) show positive correlations, especially in the 25% most reliable voxels mask, and it increases with the dimension of the embeddings from 300 to 1024. GloVe word embeddings perform better than these baselines. Finally, the contextual embeddings provided by the large language models yield even higher brain correlations.

[2] We performed exploratory analyses showing that a single value for α for all the voxels in the brain was not detrimental to the predictions of the functional data, and produced a massive gain in speed.

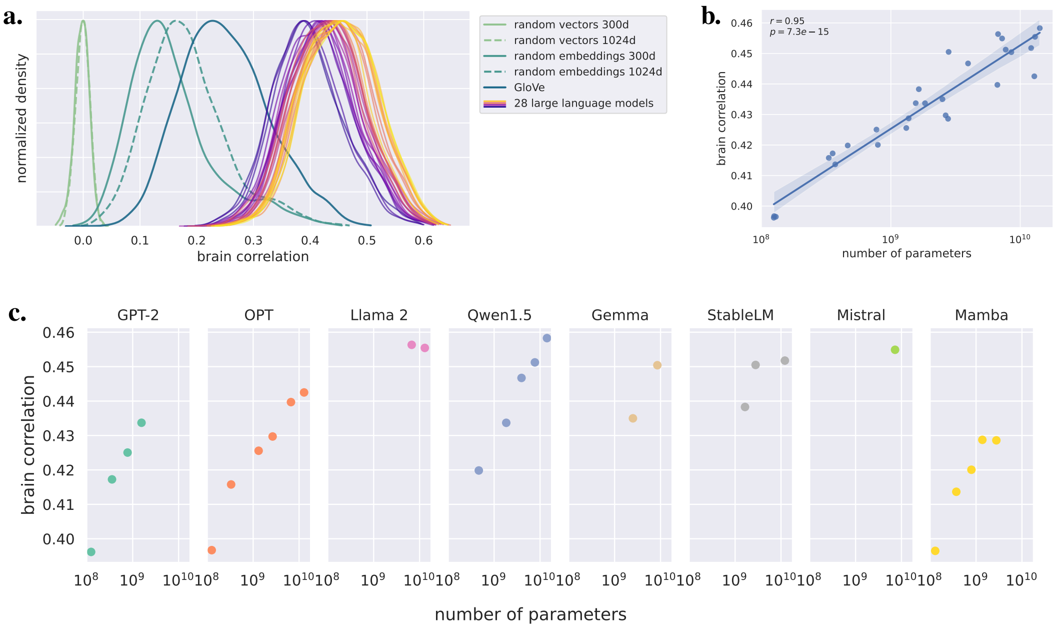

Figure 2: **Performance of various models in predicting fMRI brain time-courses**. (a) Density estimates of the distributions of r-scores obtained for all 28 large language models, the random baselines and GloVe. The densities are scaled to have the same maximum (b) Average r-score as a function of the number of parameters of the model, in log scale. Here and in the next figures, the shaded area indicates the 95% confidence interval of the slope, computed with bootstrap. (c) Same, split by models' family.

3.2 Scaling law of fMRI encoding models

Focusing on the contextual large language models, Fig. 2b shows the relationship between the size of the language models and their prediction performance, that is, the average correlation across the 25% most reliable voxels. The linear correlation between the brain correlation and the logarithm of the number of parameters is $r = 0.95, p = 7.3e - 15$. The corresponding plot for the whole volume, displayed in panel (b) of Fig. B.2, also shows a linear relationship ($r = 0.95, p = 3.2e - 14$). This finding replicates the scaling law first described by Antonello et al. (2024).
Fig. 2c details the results by the family of models. Older models like the ones from the OPT family perform worse than more recent ones like Mistral or Qwen, although within the same family the scaling law holds well in general, as exemplified by the GPT-2, OPT or Qwen1.5 families. Interestingly, the Mamba family, which is based on a recurrent neural network architecture contrary to all the other, Transformer-based, models, has similar brain scores, although they lie at the bottom of the envelope of the results (see Fig. B.3). In addition, we performed an analysis of the fit as a function of layer depth, depicted in Fig. B.4. The results confirm earlier reports by Toneva and Wehbe (2019) and Caucheteux and King (2022) that the middle layers are the most predictive ones.

Brain maps of smallest vs. largest models. Fig. 3 shows the brain correlations maps associated with the two most extreme models: GPT-2 with the smallest number of parameters and Qwen1.5-14B with the largest number of parameters. Interestingly, while the map generated by GPT-2 is quite symmetric, Qwen1.5-14B fits fMRI responses better in the left hemisphere than in the right (while overall performing better than GPT-2).

Voxel-wise sensitivity to model size. To investigate the strength of the relationship between model size and brain score in each voxel, we compute the slope of the linear regression line between the logarithm of the number of parameters and the correlation score. These slopes are displayed in Fig. 4. The strongest effects of model size are detected in the left angular gyrus, the medial prefrontal cortex and the precuneus on the medial surface of the parietal lobe. Smaller effects are detected in the middle temporal and inferior frontal gyri.

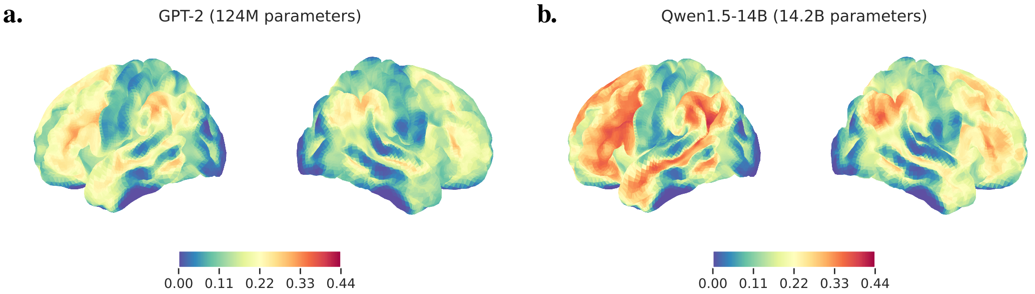

Figure 3: **Brain correlation maps associated with the smallest (a) and the largest model (b)**. These maps show the increase in r-score relative to the model using the random embedding baseline 1024d.

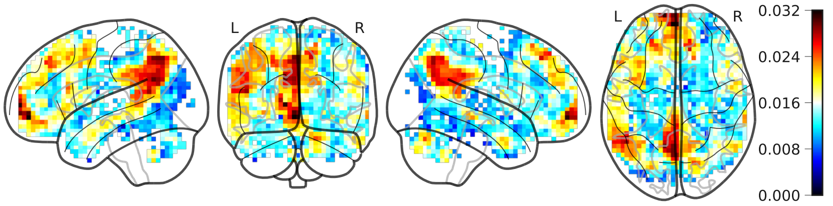

Figure 4: **Voxel-wise strength of the relationship between models' size and their predictive power**. The slopes of the linear regression between r-score and the logarithm of the number of parameters are presented on a glass brain view. For readability, only voxels with p-values smaller than 10^{-7} are shown.

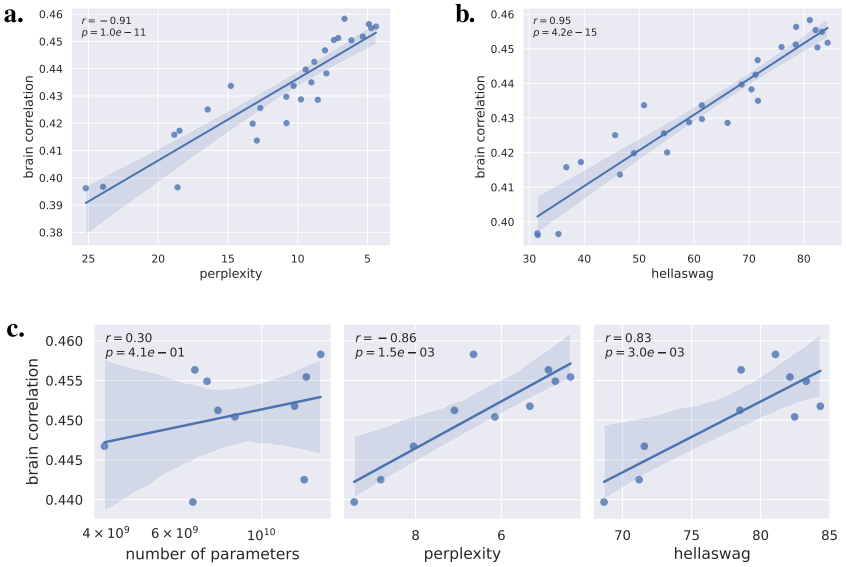

Figure 5: **Brain correlation and performance on natural language tasks**. (a) Brain correlation on the 25% most reliable voxels for all 28 large language models as of a function of perplexity on Wikitext-2 test set. Note that the x-axis is inverted, as the lower the perplexity the better the model. (b) Same with performance on the Hellaswag benchmark. The higher the better. (c) Same as Fig. 2b and (a) and (b), but focusing on the 10 largest models, with a number of parameters above 3B. See Fig. B.5 for similar plots on the whole brain volume.

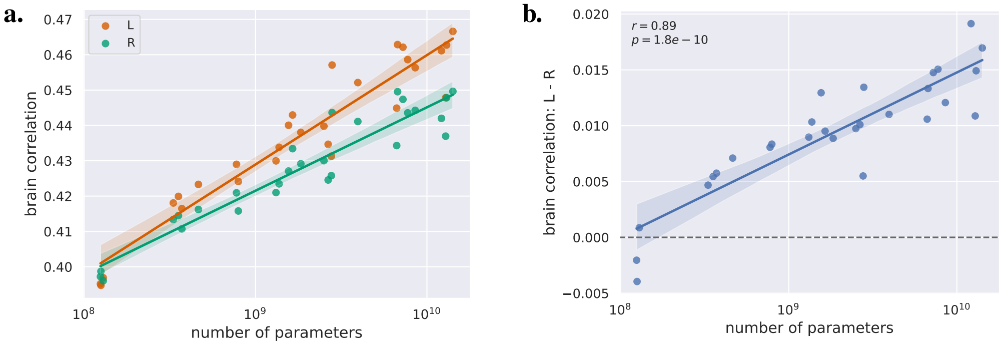

Figure 6: **Emergence of left lateralization with the size of the encoding models**. (a) Brain correlations on the 25% most reliable voxels as a function of the number of parameters, for the left hemisphere (red) and for the right hemisphere (green). (b) The difference between left and right hemispheric brain correlations also shows a scaling law.

Brain correlation and performance on natural language tasks. The number of parameters of a model is a rough proxy of its performance on language tasks. For example, OPT-13B is found to have lower performances on various natural language processing tasks than Mistral-7B which has almost half the number of parameters. Hence, we also look at measures of models' performance beyond their raw number of parameters. First we compute the perplexity of all the models on the Wikitext-2 test set (Merity et al., 2016). Second we look at the Hellaswag benchmark (Zellers et al., 2019), which aims to measure the ability of a model to understand language. This measure was found to be quite challenging for language models, and the performance of models scale on this benchmark well with the training budget, either in terms of number of parameters or number of tokens seen during training (see Touvron et al., 2023). Fig. 5 shows how brain correlation increases with better models, either as measured by lower perplexity on the Wikitext-2 test set or on the Hellaswag benchmark. Both measures exhibit strong correlation with brain fit ($r = -0.91, p = 1.1e - 11$ for perplexity and $r = 0.95, p = 4.2e - 15$ for Hellaswag). But this is particularly relevant when looking at the ten largest models, with number of parameters above 3 billions: whereas the correlation between brain score and number of parameters is no longer significant in this case ($r = 0.30, p = 0.41$), the other measures of performance display a significant correlation ($r = -0.86, p = 1.5e - 3$ for perplexity and $r = 0.83, p = 3.0e - 3$ for Hellaswag): see Fig. 5.

3.3 Left-right hemispheric asymmetry

Voxel-based analysis. The maps presented on Fig. 3 and Fig. 4 hint at left-right differences. Therefore, we plot the relationships between model size and brain scores split by hemisphere in Fig. 6a. This graphic reveals that the larger the model, the stronger the left-right asymmetry. More precisely, while the smallest models have similar r-scores both in the left and right hemisphere, the largest models yield stronger r-scores in the left one. The interaction between model size and hemisphere can be assessed by the correlation between model size and the left-right difference in r-scores, displayed in Fig. 6b. This graph shows that the difference also follows a scaling law ($r = 0.89$, $p = 1.8e^{-10}$). See Fig. B.6 for a similar analysis on the whole brain volume. Finally, as we did for the brain scores (Fig. B.4), we examined the effect of layer depth on the asymmetry. This analysis, reported on Fig. B.7, shows that the layers with the stronger fit also have the strongest left-right asymmetry.

Regions of Interest analysis. The relationships between model size and r-scores in seven regions of interest from the language network in the left hemisphere, and in their mirror-image regions in the right hemisphere, are shown on Fig. 7. Brain scores improve with model size in all regions, both in the left and in the right hemisphere. Except for pars opercularis (BA44) in the inferior frontal gyrus, and for the temporal pole (TP), a left-right asymmetry in favor of the left emerges when model size increases. The steepest effect occurs in the Angular gyrus/Temporo-parietal. This region, AG_TPJ, was already highlighted in Fig. 4 showing the slopes in individual voxels.

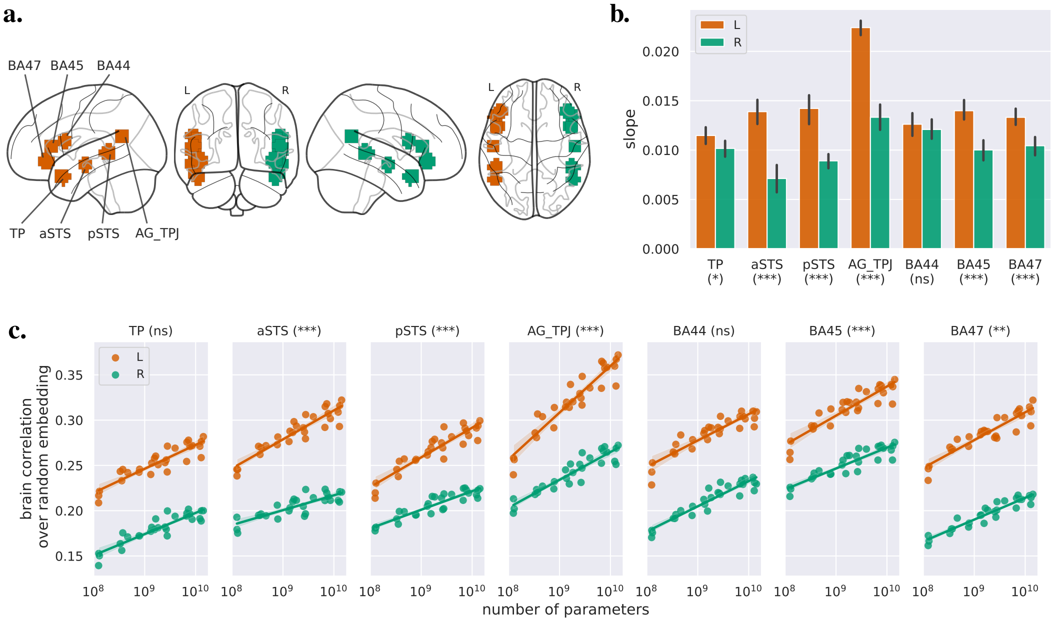

Figure 7: **Model size impact in various Regions of Interest**. (a) Locations of ROIs. (b) Slope in r-score as a function of the logarithm of the number of parameters, averaged over all voxels of a given ROI. Error bars indicate 95% confidence interval, estimated by bootstrap. The annotation below each ROI label indicates an estimate of the level of statistical significance of the difference between the slopes of the voxels of a left ROI compared to its respective right ROI (ns: non significant, $*$:$p < 0.05$, $**$:$p < 0.01$, $***$:$p < 0.001$). (c) Brain correlations over the random embedding baseline (see Fig. B.9 on page 22 for similar plots with raw brain correlations), as a function of the logarithm of the number of parameters. The annotation next to each ROI label indicates the level of statistical significance of the correlation between the difference in r-scores of the models on the left hemisphere minus the right hemisphere, as a function of the logarithm of the number of parameters, testing the interaction between hemisphere and model size. See Table A.2 for full statistics.

Relationship between signal-to-noise ratio, brain scores, and growth in asymmetry. Do large models fit the left hemisphere better than the right simply because the signal-to-noise ratio, or ceiling of explainable signal, is higher in the left voxels than in the right ones? A proxy for the explainable signal is the model-free inter-subject correlation (ISC). Fig. B.1 shows that the ISC indeed tends to be stronger on the left. To determine if this could explain our findings, we conducted several analyses presented on Fig. B.8 and Fig. B.9. First, we computed "normalized r-scores" by dividing raw r-scores by the ISC in each voxel. Panels (a) and (b) of Fig. B.8 display the relationship between these normalized brain correlations and model size. The left-right asymmetry previously observed with raw r-scores on Fig. 6 still holds. Next, using the parcels from the Harvard-Oxford atlas, we plot the relationship between ISC, brain correlations and their asymmetry (Fig. B.8, bottom panels). Although ISC and brain correlation correlate (panel c), the left-right difference in slope of brain correlation as a function of model size does not covary with the interhemispheric difference in ISC (panel d). Finally, we computed the ISC in our Regions of Interest. Fig. B.9 suggests that while differences in ISC partly explain the average brain score difference, they do not explain the increase in difference between left and right hemispheres, across models.

Impact of model training. In order to assess the impact of model training on the left-right asymmetry, we compared r-scores for randomly initialized, untrained models, and for trained models, from the GPT-2 and the Qwen1.5 families. Fig. B.10a shows that, with training, brain correlations get better on the left hemisphere compared to the right one. Moreover, while the left-right score difference increases with the number of parameters for trained models, this relationship breaks down and is flat in the case of the untrained models. Another way to assess the influence of model training is to fit the same LLM at various stages of training. The Pythia family (Biderman et al., 2023) provides many intermediate checkpoints during training, from the untrained model, randomly initialized, to the full model, trained on one epoch on the training set of 300B tokens from the Pile dataset. Here we consider Pythia-6.9B, with 32 layers and 4096 dimensions. Fig. B.10b shows the impact of training on brain correlations. The model's fit improves as training proceeds and the left-right asymmetry, originality biased towards the right hemisphere, increases, reaching a plateau favoring the left hemisphere.

3.4 Extension to other languages

As left dominance is universal (see e.g. Malik-Moraleda et al., 2022; it is even attested in sign language, Poizner et al., 1987), we wanted to check if our result holds for other languages. We therefore applied our approach to Chinese and French data provided in *Le Little Prince* dataset (considering all 35 Chinese participants and all 28 French participants).

We first computed inter-subjects correlations. Their distributions and the corresponding maps are displayed on Fig.B.11 and Fig.B.12 panels (a) and (b). The correlation values are lower than for English (Fig.B.1), but the most reliable voxels encompass the same brain regions. Panels (d) and (e) reporting correlations in regions from the Harvard-Oxford atlas (shown in panel (c)) and their left-right difference qualitatively replicate the previous observations in English results, that is, left-right asymmetries are detected in the same regions.

Although much fewer LLMs are available than for English, some models on the Hugging Face hub were trained on Chinese or French data. We considered 10 models for Chinese, ranging from 12M to 14B parameters, and 4 models for French, ranging from 124M to 7B parameters (see panel (f)). The relationships between model size and r-scores are presented in panels (g), (h) and (i) of Fig. B.11 and Fig. B.12. They confirm the scaling law, and the emergence of the left-right hemispheric asymmetry in two languages different from English.

3.5 Individual analyses

The analyses presented above were performed on data averaged across individuals. It is important to verify if the emergence of asymmetry holds at the individual level or is an artifact of averaging. Because of limitations in time and computational power available to us, we could only analyze five participants on a subset of models. To avoid any bias, we selected the first 5 English participants. The results, presented in Fig. B.13, show that three of them present a significant increase in asymmetry ($p < 0.05$) when considering the full brain (panel c), and four when considering the 10% voxels with the highest r-scores in each hemisphere (panel e).

4 Discussion & Conclusion

By manipulating the size of artificial neural language models used to fit fMRI data of naturalistic language comprehension, we observed: (1) a linear relationship between the logarithm of the number of parameters of models and their ability to predict the fMRI time-courses (Fig. 2) and (2) a left-right asymmetry emerging when encoding models are based on increasingly complex models (Fig. 6).

The first observation replicates the finding of Antonello et al. (2024) who described a scaling law between model size and brain score, extending to brain data the scaling laws observed between model size and performance on various NLP tasks (Kaplan et al., 2020). Here, we generalize their result to a different dataset that includes three languages, and using a larger variety of models and families that notably include a non-Transformer, Mamba.

The scaling law breaks down when focusing on the largest models, above 3B parameters. Yet, in this range, indices assessing the performance of the model on NLP tasks are still predictive of brain score (Fig. 5). The relationship between neural network models performance in NLP tasks and brain scores, was also investigated by Schrimpf et al. (2021) and by Caucheteux and King (2022). Both teams reported that brain scores generally improved as the performance in the next word prediction task increased, extending to the field of language processing results that were found in the visual domain by Schrimpf et al. (2020) or in the auditory domain by Kell et al. (2018). Caucheteux and King (2022) found that brain scores reached a plateau, and even dropped somewhat (see their Fig.2g) which might be due to an overspecialization for the next word prediction task in their study (Caucheteux et al., 2023).

Our second observation is the emergence of an asymmetry with increasing model size, a finding that has not been reported in the literature [3]. A quick but vague explanation is that larger models better capture language representations in the left hemisphere. It begs the question of which representations are improved in larger models relative to smaller ones. For example, is it lexical, syntactic, semantic, pragmatic or world knowledge? The present work calls for detailed comparisons of the features discovered by large vs small language models, and how and where this translates into better fMRI prediction.

One can attempt to perform inverse inference, that is, try to infer which processes are involved from the brain areas highlighted by our analyses, keeping in mind the pitfalls of such an approach (Poldrack, 2011). The cortical areas where model size has the strongest impact are the Angular gyrus, the Precuneus and the medial prefrontal cortex (mPFC). These regions are also those where the effects of training a (small) network are the strongest Pasquiou et al. (2022) and were fit by models trained on semantic but not on syntax by Pasquiou et al. (2023). These regions are not specific to language, e.g. they are part of the default mode network, but are involved in the highest levels of language comprehension (Simony et al., 2016; Chang et al., 2022). The mPFC and Precuneus are known to be sensitive to discourse coherence (Ferstl and von Cramon, 2001; Xu et al., 2005). The Angular Gyrus is also considered part of the semantic system (Seghier et al., 2010; Binder and Desai, 2011; Price et al., 2015; Kuhnke et al., 2023). This suggests that the main effect of increasing model size is to improve the model capabilities at the semantic and pragmatic levels. The analysis by regions of interest revealed that the asymmetry holds in most regions of the core language network, except pars opercularis (BA44) and the Temporal Pole. The left BA44 has been associated with syntax (Zaccarella and Friederici, 2016) and/or speech processing (Matchin and Hickok, 2020). The temporal poles, both on the left and on the right, are linked to semantic processing (Pobric et al., 2010; Pylkkänen, 2019) and have been designated as an amodal semantic hub by Patterson and Lambon Ralph (2016) (but see Snowden et al., 2018).

It is remarkable that in all regions of interest, even in the right hemisphere, the largest models' fits always improve over the smallest models (see Fig.7). It has been known for long that the right hemisphere has some language capacity (Bradshaw et al., 2017), which can manifest in split brain patients or in patients with lesions in the left hemisphere (Vigneau et al., 2011). The right hemisphere has been associated with speech processing, especially prosody, usually considered to be processed in the right temporal lobe (Wildgruber et al., 2006), as well as with high-level aspects of language understanding involved in the comprehension of metaphors or jokes (Jung-Beeman, 2005; Bookheimer, 2002). More work will be needed to determine which aspects of LLMs allow them to fit these regions.

Our main analyses were performed on fMRI data averaged across participants because of computational power limitations. We report preliminary analyses on 5 participants showing that the emergence of asymmetry holds at the individual level (see Fig. B.13). Nevertheless there is an important variability between subjects in brain correlations, in the difference between left hemispheric vs. right hemispheric average brain correlations, and in the slope of the left-right difference. It would be interesting for future work to assess the reliability of these measures, and to compare them with independent assessments of individual language hemispheric dominance. Unfortunately, such measurements are not provided in the fMRI dataset that we use.

An interesting question concerns the evolution of lateralization during the training process of large language models, either by training such a model from scratch or by having access to checkpoints during the training (see Antonello et al., 2024; Pasquiou et al., 2022, for first attempts). In humans, it seems that language processing in the brain starts bilaterally and then becomes progressively lateralized over time (Szaflarski et al., 2006; Olulade et al., 2020; Ozernov-Palchik et al., 2024), although some studies have found very early lateralization (Witelson and Pallie, 1973; Wood et al., 2004). Our preliminary exploration with the Pythia-6.9B model (Fig. B.10) reveals that the left-right asymmetry emerges during the training process. This leaves open the questions of which representations improved by learning are responsible for this asymmetry, and whether parallels with the development of language acquisition can be drawn.

[3] Note that the growing asymmetry with model size goes beyond showing a left-right difference in a single model, which could be explained by signal-to-noise ratio asymmetry (see, e.g., Caucheteux and King, 2022, Fig. 2d)

5 Acknowledgments

We would like to sincerely thank all four anonymous reviewers, whose constructive feedback significantly contributed to the improvement of the paper. Many thanks also to Yair Lakretz, Emmanuel Chemla, and all the participants of the Linguae ML seminar at École Normale Supérieure.

References

Antonello, R., Vaidya, A., and Huth, A. (2024). Scaling laws for language encoding models in fMRI. *Advances in Neural Information Processing Systems*, 36.

Bai, J., Bai, S., Chu, Y., Cui, Z., Dang, K., Deng, X., Fan, Y., Ge, W., Han, Y., Huang, F., et al. (2023). Qwen technical report. *arXiv preprint arXiv:2309.16609*.

Bellagente, M., Tow, J., Mahan, D., Phung, D., Zhuravinskyi, M., Adithyan, R., Baicoianu, J., Brooks, B., Cooper, N., Datta, A., et al. (2024). Stable lm 2 1.6 b technical report. *arXiv preprint arXiv:2402.17834*.

Biderman, S., Schoelkopf, H., Anthony, Q. G., Bradley, H., O'Brien, K., Hallahan, E., Khan, M. A., Purohit, S., Prashanth, U. S., Raff, E., et al. (2023). Pythia: A suite for analyzing large language models across training and scaling. In *International Conference on Machine Learning*, pages 2397–2430. PMLR.

Binder, J. R. and Desai, R. H. (2011). The neurobiology of semantic memory. *Trends in Cognitive Sciences*, 15(11):527–536.

Binder, J. R., Swanson, S. J., Hammeke, T. A., Morris, G. L., Mueller, W. M., Fischer, M., Benbadis, S., Frost, J. A., Rao, S. M., and Haughton, V. M. (1996). Determination of language dominance using functional MRI: a comparison with the Wada test. *Neurology*, 46(4):978–984.

Bookheimer, S. (2002). Functional MRI of Language: New Approaches to Understanding the Cortical Organization of Semantic Processing. *Annual Review of Neuroscience*, 25(1):151–188.

Bradshaw, A. R., Thompson, P. A., Wilson, A. C., Bishop, D. V., and Woodhead, Z. V. (2017). Measuring language lateralisation with different language tasks: a systematic review. *PeerJ*, 5:e3929.

Broca, P. (1865). Sur le siège de la faculté du langage articulé. *Bulletins et Mémoires de la Société d'Anthropologie de Paris*, 6(1):377–393.

Caucheteux, C., Gramfort, A., and King, J.-R. (2021). Disentangling syntax and semantics in the brain with deep networks. In *International conference on machine learning*, pages 1336–1348. PMLR.

Caucheteux, C., Gramfort, A., and King, J.-R. (2023). Evidence of a predictive coding hierarchy in the human brain listening to speech. *Nature Human Behaviour*, 7(3):430–441.

Caucheteux, C. and King, J.-R. (2022). Brains and algorithms partially converge in natural language processing. *Communications biology*, 5(1):1–10.

Chang, C. H. C., Nastase, S. A., and Hasson, U. (2022). Information flow across the cortical timescale hierarchy during narrative construction. *Proceedings of the National Academy of Sciences*, 119(51):e2209307119. Publisher: Proceedings of the National Academy of Sciences.

Dax, M. D. (1865). Lésions de la moitié gauche de l'encéphale coïncidant avec l'oubli des signes de la pensée: Lu au Congrès méridional tenu à Montpellier en 1836, par le docteur Marc Dax. *Gazette Hebdomadaire de Médecine et de Chirurgie*, 17:259–260.

Ferstl, E. C. and von Cramon, D. Y. (2001). The role of coherence and cohesion in text comprehension: an event-related fMRI study. *Cognitive Brain Research*, 11(3):325–340.

Gazzaniga, M. S. and Sperry, R. W. (1967). Language after section of the cerebral commissures. *Brain*, 90(1):131–148. Publisher: Oxford University Press.

Glover, G. H. (1999). Deconvolution of impulse response in event-related BOLD fMRI. *Neuroimage*, 9(4):416–429.

Gu, A. and Dao, T. (2023). Mamba: Linear-time sequence modeling with selective state spaces. *arXiv preprint arXiv:2312.00752*.

Hausmann, M., Brysbaert, M., van der Haegen, L., Lewald, J., Specht, K., Hirnstein, M., Willemin, J., Barton, J., Buchilly, D., Chmetz, F., Roch, M., Brederoo, S., Dael, N., and Mohr, C. (2019). Language lateralisation measured across linguistic and national boundaries. *Cortex*, 111:134–147.

Heer, W. A. d., Huth, A. G., Griffiths, T. L., Gallant, J. L., and Theunissen, F. E. (2017). The Hierarchical Cortical Organization of Human Speech Processing. *Journal of Neuroscience*, 37(27):6539–6557. Publisher: Society for Neuroscience Section: Research Articles.

Hunter, J. D. (2007). Matplotlib: A 2D graphics environment. *Computing in Science & Engineering*, 9(3):90–95.

Huth, A. G., De Heer, W. A., Griffiths, T. L., Theunissen, F. E., and Gallant, J. L. (2016). Natural speech reveals the semantic maps that tile human cerebral cortex. *Nature*, 532(7600):453–458.

Jain, S. and Huth, A. (2018). Incorporating context into language encoding models for fmri. *Advances in neural information processing systems*, 31.

Jiang, A. Q., Sablayrolles, A., Mensch, A., Bamford, C., Chaplot, D. S., Casas, D. d. l., Bressand, F., Lengyel, G., Lample, G., Saulnier, L., et al. (2023). Mistral 7B. *arXiv preprint arXiv:2310.06825*.

Josse, G. and Tzourio-Mazoyer, N. (2004). Hemispheric specialization for language. *Brain Research Reviews*, 44(1):1–12.

Jung-Beeman, M. (2005). Bilateral brain processes for comprehending natural language. *Trends in Cognitive Sciences*, 9(11):512–518.

Just, M. A., Carpenter, P. A., Keller, T. A., Eddy, W. F., and Thulborn, K. R. (1996). Brain activation modulated by sentence comprehension. *Science*, 274(5284):114–116.

Kaplan, J., McCandlish, S., Henighan, T., Brown, T. B., Chess, B., Child, R., Gray, S., Radford, A., Wu, J., and Amodei, D. (2020). Scaling laws for neural language models. *arXiv preprint arXiv:2001.08361*.

Kauf, C., Tuckute, G., Levy, R., Andreas, J., and Fedorenko, E. (2024). Lexical-Semantic Content, Not Syntactic Structure, Is the Main Contributor to ANN-Brain Similarity of fMRI Responses in t he Language Network. *Neurobiology of Language*, 5(1):7–42.

Kell, A. J., Yamins, D. L., Shook, E. N., Norman-Haignere, S. V., and McDermott, J. H. (2018). A task-optimized neural network replicates human auditory behavior, predicts brain responses, and reveals a cortical processing hierarchy. *Neuron*, 98(3):630–644.

Kuhnke, P., Chapman, C. A., Cheung, V. K. M., Turker, S., Graessner, A., Martin, S., Williams, K. A., and Hartwigsen, G. (2023). The role of the angular gyrus in semantic cognition: a synthesis of five functional neuroimaging studies. *Brain Structure and Function*, 228(1):273–291.

Landauer, T. K. and Dumais, S. T. (1997). A solution to Plato's problem: The latent semantic analysis theory of acquisition, induction, and representation of knowledge. *Psychological review*, 104(2):211. Publisher: American Psychological Association.

Lerner, Y., Honey, C. J., Silbert, L. J., and Hasson, U. (2011). Topographic Mapping of a Hierarchy of Temporal Receptive Windows Using a Narrated Story. *Journal of Neuroscience*, 31(8):2906–2915.

Li, J., Bhattasali, S., Zhang, S., Franzluebbers, B., Luh, W.-M., Spreng, R. N., Brennan, J. R., Yang, Y., Pallier, C., and Hale, J. (2022). Le petit prince multilingual naturalistic fmri corpus. *Scientific data*, 9(1):530.

Malik-Moraleda, S., Ayyash, D., Gallée, J., Affourtit, J., Hoffmann, M., Mineroff, Z., Jouravlev, O., and Fedorenko, E. (2022). An investigation across 45 languages and 12 language families reveals a universal language network. *Nature Neuroscience*, 25(8):1014–1019.

Manning, L. and Thomas-Antérion, C. (2011). Marc Dax and the discovery of the lateralisation of language in the left cerebral hemisphere. *Revue Neurologique*, 167(12):868–872.

Matchin, W. and Hickok, G. (2020). The Cortical Organization of Syntax. *Cerebral Cortex*, 30(3):1481–1498.

McKinney, W. et al. (2010). Data structures for statistical computing in python. In *Proceedings of the 9th Python in Science Conference*, volume 445, pages 51–56. Austin, TX.

Merity, S., Xiong, C., Bradbury, J., and Socher, R. (2016). Pointer sentinel mixture models. *arXiv preprint arXiv:1609.07843*.

Olulade, O. A., Seydell-Greenwald, A., Chambers, C. E., Turkeltaub, P. E., Dromerick, A. W., Berl, M. M., Gaillard, W. D., and Newport, E. L. (2020). The neural basis of language development: Changes in lateralization over age. *Proceedings of the National Academy of Sciences*, 117(38):23477–23483.

Ozernov-Palchik, O., O'Brien, A. M., Lee, E. J., Richardson, H., Romeo, R., Lipkin, B., Small, H., Capella, J., Nieto-Castanon, A., Saxe, R., Gabrieli, J. D. E., and Fedorenko, E. (2024). Precision fMRI reveals that the language network exhibits adult-like left-hemispheric lateralization by 4 years of age.

Pallier, C., Devauchelle, A.-D., and Dehaene, S. (2011). Cortical representation of the constituent structure of sentences. *Proceedings of the National Academy of Sciences*, 108(6):2522–2527.

Pasquiou, A., Lakretz, Y., Hale, J., Thirion, B., and Pallier, C. (2022). Neural language models are not born equal to fit brain data, but training helps. *arXiv preprint arXiv:2207.03380*.

Pasquiou, A., Lakretz, Y., Thirion, B., and Pallier, C. (2023). Information-Restricted Neural Language Models Reveal Different Brain Regions' Sensitivity to Semantics, Syntax, and Context. *Neurobiology of Language*, 4(4):611–636.

Paszke, A., Gross, S., Massa, F., Lerer, A., Bradbury, J., Chanan, G., Killeen, T., Lin, Z., Gimelshein, N., Antiga, L., et al. (2019). Pytorch: An imperative style, high-performance deep learning library. *Advances in neural information processing systems*, 32.

Patterson, K. and Lambon Ralph, M. A. (2016). The Hub-and-Spoke Hypothesis of Semantic Memory. In *Neurobiology of Language*, pages 765–775. Elsevier.

Pedregosa, F., Varoquaux, G., Gramfort, A., Michel, V., Thirion, B., Grisel, O., Blondel, M., Prettenhofer, P., Weiss, R., Dubourg, V., et al. (2011). Scikit-learn: Machine learning in Python. *Journal of machine learning research*, 12(Oct):2825–2830.

Penfield, W. and Roberts, L. (1959). *Speech and Brain Mechanisms*. Princeton University Press, Princeton, NJ.

Pennington, J., Socher, R., and Manning, C. D. (2014). Glove: Global vectors for word representation. In *Proceedings of the 2014 conference on empirical methods in natural language processing (EMNLP)*, pages 1532–1543.

Pobric, G., Jefferies, E., and Lambon Ralph, M. A. (2010). Amodal semantic representations depend on both anterior temporal lobes: Evidence from repetitive transcranial magnetic stimulation. *Neuropsychologia*, 48(5):1336–1342.

Poizner, H., Bellugi, U., and Klima, E. (1987). *What the Hand reveals about the Brain*. MIT Press, Cambridge, MA.

Poldrack, R. A. (2011). Inferring mental states from neuroimaging data: From reverse inference to large-scale decoding. *Neuron*, 72(5):692–697.

Price, A. R., Bonner, M. F., Peelle, J. E., and Grossman, M. (2015). Converging evidence for the neuroanatomic basis of combinatorial semantics in the angular gyrus. *Journal of Neuroscience*, 35(7):3276–3284.

Pylkkänen, L. (2019). The neural basis of combinatory syntax and semantics. *Science*, 366(6461):62–66.

Radford, A., Wu, J., Child, R., Luan, D., Amodei, D., Sutskever, I., et al. (2019). Language models are unsupervised multitask learners. *OpenAI blog*, 1(8):9.

Schrimpf, M., Blank, I. A., Tuckute, G., Kauf, C., Hosseini, E. A., Kanwisher, N., Tenenbaum, J. B., and Fedorenko, E. (2021). The neural architecture of language: Integrative modeling converges on predictive processing. *Proceedings of the National Academy of Sciences*, 118(45).

Schrimpf, M., Kubilius, J., Hong, H., Majaj, N. J., Rajalingham, R., Issa, E. B., Kar, K., Bashivan, P., Prescott-Roy, J., Geiger, F., et al. (2020). Brain-score: Which artificial neural network for object recognition is most brain-like? *BioRxiv*, page 407007.

Seabold, S. and Perktold, J. (2010). statsmodels: Econometric and statistical modeling with python. In *9th Python in Science Conference*.

Seghier, M. L., Fagan, E., and Price, C. J. (2010). Functional subdivisions in the left angular gyrus where the semantic system meets and diverges from the default network. *The Journal of Neuroscience: The Official Journal of the Society for Neuroscience*, 30(50):16809–16817.

Simony, E., Honey, C. J., Chen, J., Lositsky, O., Yeshurun, Y., Wiesel, A., and Hasson, U. (2016). Dynamic reconfiguration of the default mode network during narrative comprehension. *Nature Communications*, 7(1):12141. Number: 1 Publisher: Nature Publishing Group.

Snowden, J. S., Harris, J. M., Thompson, J. C., Kobylecki, C., Jones, M., Richardson, A. M., and Neary, D. (2018). Semantic dementia and the left and right temporal lobes. *Cortex*, 107:188–203.

Stromswold, K., Caplan, D., Alpert, N., and Rauch, S. (1996). Localization of syntactic comprehension by positron emission tomography. *Brain and language*, 52(3):452–473.

Szaflarski, J. P., Holland, S. K., Schmithorst, V. J., and Byars, A. W. (2006). fMRI study of language lateralization in children and adults. *Human brain mapping*, 27(3):202–212.

Team, G., Mesnard, T., Hardin, C., Dadashi, R., Bhupatiraju, S., Pathak, S., Sifre, L., Rivière, M., Kale, M. S., Love, J., et al. (2024). Gemma: Open models based on gemini research and technology. *arXiv preprint arXiv:2403.08295*.

Toneva, M. and Wehbe, L. (2019). Interpreting and improving natural-language processing (in machines) with natural language-processing (in the brain). *Advances in neural information processing systems*, 32.

Touvron, H., Martin, L., Stone, K., Albert, P., Almahairi, A., Babaei, Y., Bashlykov, N., Batra, S., Bhargava, P., Bhosale, S., et al. (2023). Llama 2: Open foundation and fine-tuned chat models. *arXiv preprint arXiv:2307.09288*.

Tzourio-Mazoyer, N., Perrone-Bertolotti, M., Jobard, G., Mazoyer, B., and Baciu, M. (2017). Multifactorial modulation of hemispheric specialization and plasticity for language in healthy and pathological conditions: A review. *Cortex*, 86:314–339.

Van Der Walt, S., Colbert, S. C., and Varoquaux, G. (2011). The numpy array: a structure for efficient numerical computation. *Computing in Science & Engineering*, 13(2):22.

Vaswani, A., Shazeer, N., Parmar, N., Uszkoreit, J., Jones, L., Gomez, A. N., Kaiser, Ł., and Polosukhin, I. (2017). Attention is all you need. *Advances in neural information processing systems*, 30.

Vigneau, M., Beaucousin, V., Hervé, P.-Y., Jobard, G., Petit, L., Crivello, F., Mellet, E., Zago, L., Mazoyer, B., and Tzourio-Mazoyer, N. (2011). What is right-hemisphere contribution to phonological, lexico-semantic, and sentence processing? *NeuroImage*, 54(1):577–593.

Wada, J. and Rasmussen, T. (1960). Intracarotid Injection of Sodium Amytal for the Lateralization of Cerebral Speech Dominance: Experimental and Clinical Observations. *Journal of Neurosurgery*, 17(2):266–282. Publisher: Journal of Neurosurgery Publishing Group Section: Journal of Neurosurgery.

Waskom, M. L. (2021). seaborn: statistical data visualization. *Journal of Open Source Software*, 6(60):3021.

Wernicke, C. (1874). *Der aphasische Symptomencomplex: eine psychologische Studie auf anatomischer Basis*. Cohn & Weigert.

Wildgruber, D., Ackermann, H., Kreifelts, B., and Ethofer, T. (2006). Cerebral processing of linguistic and emotional prosody: fMRI studies. *Progress in brain research*, 156:249–268. Publisher: Elsevier.

Witelson, S. F. and Pallie, W. (1973). Left hemisphere specialization for language in the newborn: Neuroanatomical evidence of asymmetry. *Brain*, 96(3):641–646.

Wolf, T., Debut, L., Sanh, V., Chaumond, J., Delangue, C., Moi, A., Cistac, P., Rault, T., Louf, R., Funtowicz, M., et al. (2020). Transformers: State-of-the-art natural language processing. In *Proceedings of the 2020 conference on empirical methods in natural language processing: system demonstrations*, pages 38–45.

Wood, A. G., Harvey, A. S., Wellard, R. M., Abbott, D., Anderson, V., Kean, M., Saling, M., and Jackson, G. D. (2004). Language cortex activation in normal children. *Neurology*, 63(6):1035–1044.

Xu, J., Kemeny, S., Park, G., Frattali, C., and Braun, A. (2005). Language in context: emergent features of word, sentence, and narrative comprehension. *NeuroImage*, 25(3):1002–1015.

Zaccarella, E. and Friederici, A. D. (2016). The neurobiological nature of syntactic hierarchies. *Neuroscience & Biobehavioral Reviews*.

Zaccarella, E., Schell, M., and Friederici, A. D. (2017). Reviewing the functional basis of the syntactic Merge mechanism for language: A coordinate-based activation likelihood estimation meta-analysis. *Neuroscience & Biobehavioral Reviews*, 80:646–656.

Zellers, R., Holtzman, A., Bisk, Y., Farhadi, A., and Choi, Y. (2019). Hellaswag: Can a machine really finish your sentence? *arXiv preprint arXiv:1905.07830*.

Zhang, S., Roller, S., Goyal, N., Artetxe, M., Chen, M., Chen, S., Dewan, C., Diab, M., Li, X., Lin, X. V., et al. (2022). Opt: Open pre-trained transformer language models. *arXiv preprint arXiv:2205.01068*.

A Supplementary Tables

Table A.1: List of the 28 English large language models included in the study, grouped by family.

model name	$n_{\text{parameters}}$	n_{layers}	n_{neurons}
gpt2	124M	12	768
gpt2-medium	355M	24	1024
gpt2-large	774M	36	1280
gpt2-xl	1.56B	48	1600
opt-125m	125M	12	768
opt-350m	331M	24	1024
opt-1.3b	1.32B	24	2048
opt-2.7b	2.65B	32	2560
opt-6.7b	6.66B	32	4096
opt-13b	12.9B	40	5120
Llama-2-7b-hf	6.74B	32	4096
Llama-2-13b-hf	13.02B	40	5120
Qwen1.5-0.5B	464M	24	1024
Qwen1.5-1.8B	1.84B	24	2048
Qwen1.5-4B	3.95B	40	2560
Qwen1.5-7B	7.72B	32	4096
Qwen1.5-14B	14.17B	40	5120
gemma-2b	2.51B	18	2048
gemma-7b	8.54B	28	3072
stablelm-2-1_6b	1.64B	24	2048
stablelm-3b-4e1t	2.80B	32	2560
stablelm-2-12b	12.14B	40	5120
Mistral-7B-v0.1	7.24B	32	4096
mamba-130m-hf	129M	24	768
mamba-370m-hf	372M	48	1024
mamba-790m-hf	793M	48	1536
mamba-1.4b-hf	1.37B	48	2048
mamba-2.8b-hf	2.77B	64	2560

Table A.2: **Per ROI tests of the interaction between hemisphere and model size**. The first column is the name of each ROI. The second column gives the p-value of the two sample t-test between the set of slopes of all the voxels of the left vs. the right corresponding ROI, whose means and 95% confidence intervals are depicted in Fig. 7b. The third column presents the correlation between the difference in performance of the models (the r-scores) on the left hemisphere minus the right hemisphere as a function of the logarithm of the number of parameters, as described in Fig. 7c. The last column gives the p-value of the correlation. These two measures of interaction lead to the same conclusions: the interaction is not significant for BA44 and TP (marginal in the latter case), and highly significant for all the other ROIs, namely aSTS, pSTS, AG_TPJ, BA45 and BA47.

ROI	p-value of two sample t-test	correlation L-R vs. $\log(n_{\text{parameters}})$	p-value
TP	4.1e-02	0.36	6.2e-02
aSTS	7.3e-11	0.85	1.0e-08
pSTS	3.5e-09	0.82	1.2e-07
AG_TPJ	9.3e-22	0.84	1.7e-08
BA44	4.8e-01	0.15	4.6e-01
BA45	5.7e-07	0.73	9.4e-06
BA47	1.4e-05	0.56	1.9e-03

B Supplementary Figures

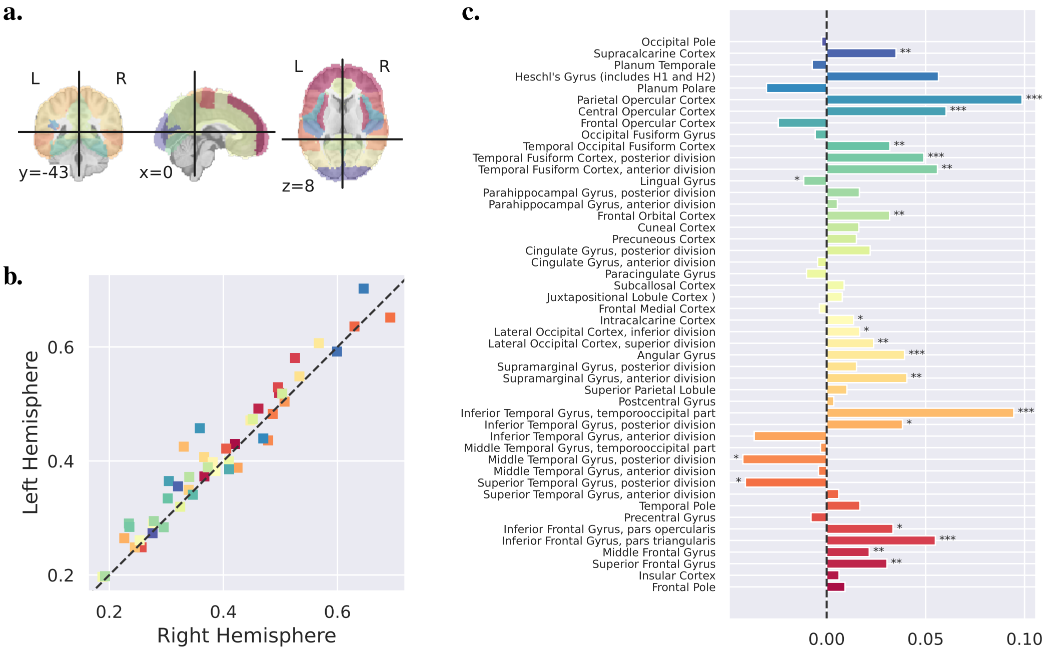

Figure B.1: **Inter-subjects correlations (model free) in homologous cortical regions of the left and right hemispheres**. (a) The 48 cortical areas from nilearn's `cort-maxprob-thr0-2mm` version of the Harvard-Oxford atlas. (b) Relationship between right and left inter-subjects correlations (dots correspond to regions from the atlas) (c) Differences in correlations between left and right regions. The number of stars next to each bar indicates an estimate of the level of statistical significance, assessed with a two-sample t-test ($*$:$p < 0.05$, $**$:$p < 0.01$, $***$:$p < 0.001$).

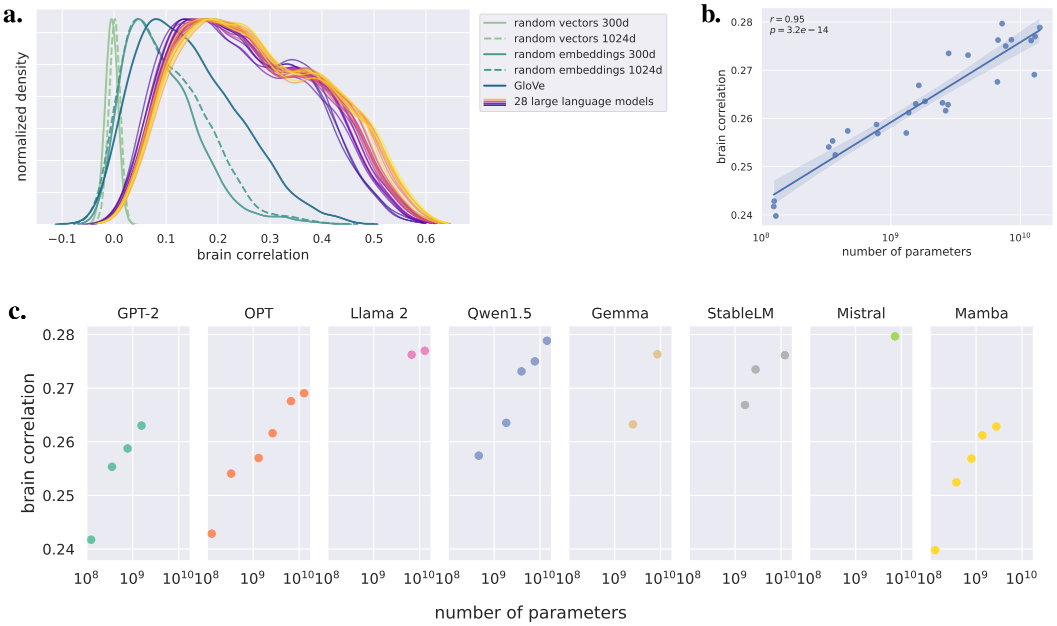

Figure B.2: **Performance of various models in predicting fMRI brain time-courses**. Same as Fig. 2, but for the whole brain volume.

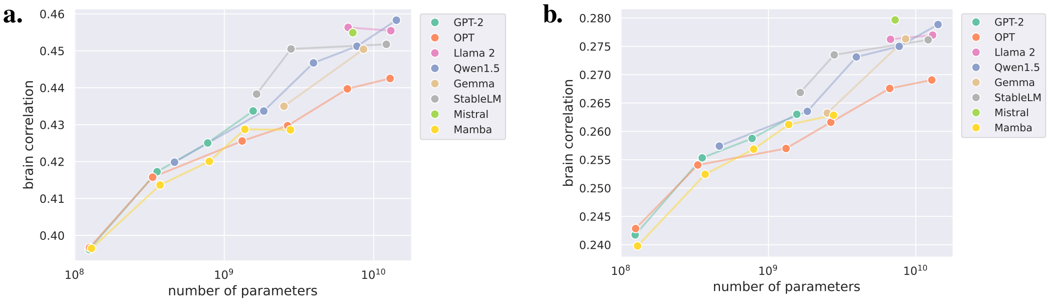

Figure B.3: **Scaling law of fMRI encoding models, by family**. (a) Average over the 25% most reliable voxels (b) Average over the whole brain volume.

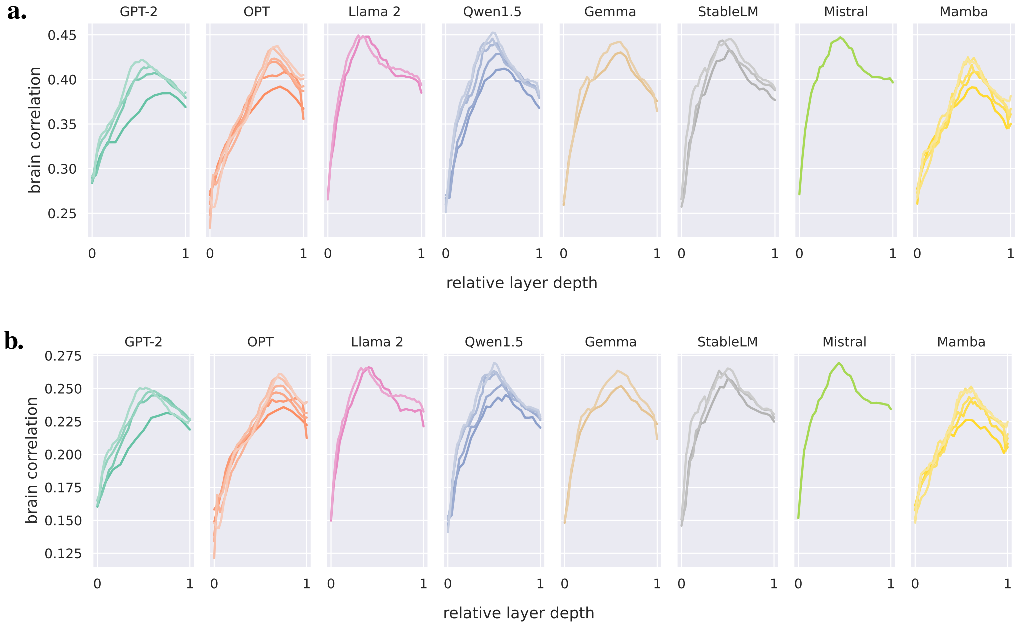

Figure B.4: **Brain correlation as a function of the relative layer depth, split by family**. The relative layer depth corresponds to the depth of a given layer relative to the input and output layers: the first layer is the non-contextual embedding layer, at position 0, and the last hidden layer is at position 1. Considering (a) the 25% most reliable voxels or (b) the whole brain volume.

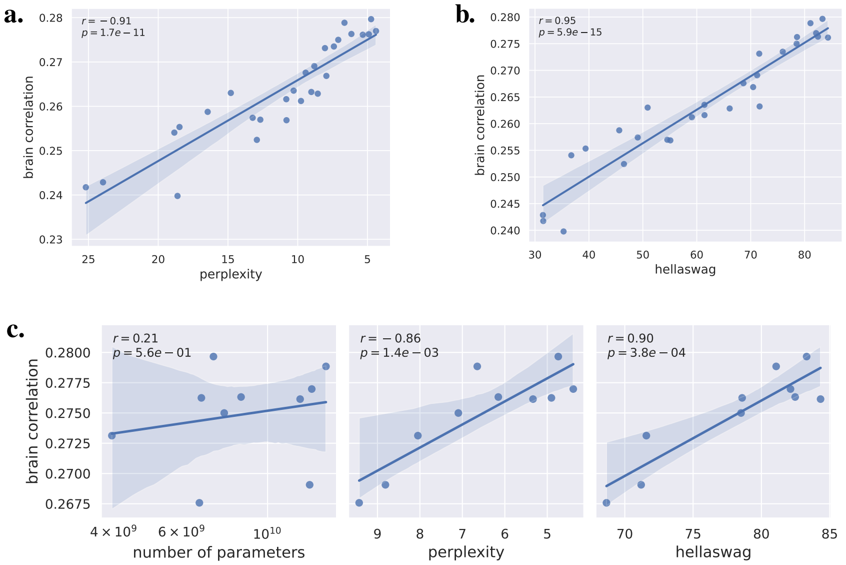

Figure B.5: **Brain correlation and performance on natural language tasks**. Same as Fig. 5, but for the whole brain volume.

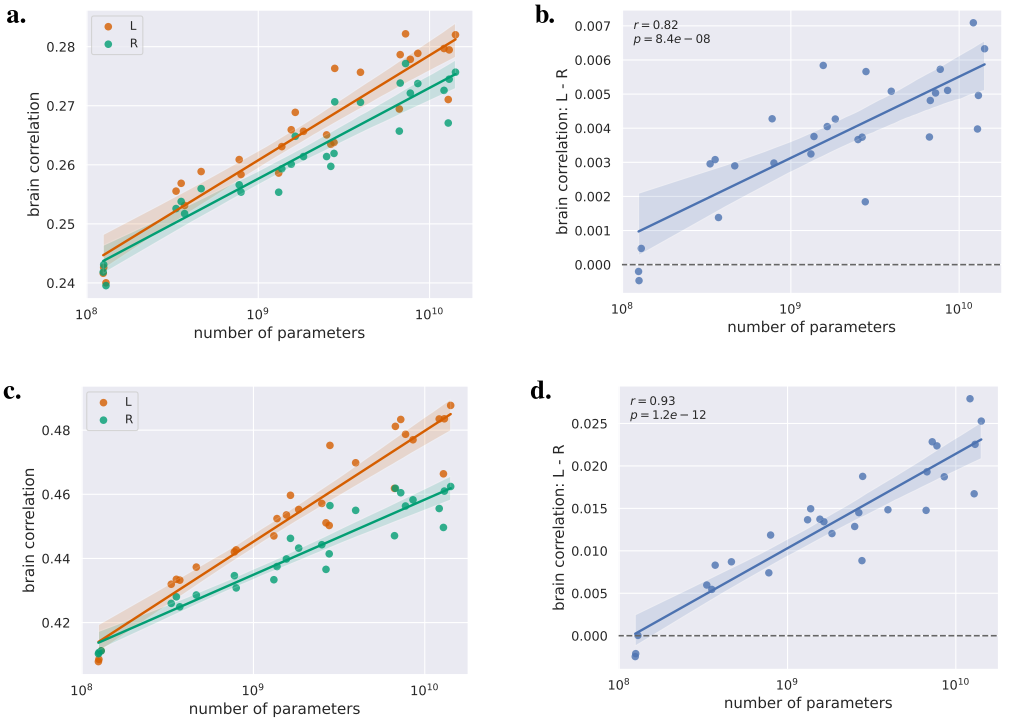

Figure B.6: **Emergence of left lateralization with the size of the encoding models**. Same as Fig. 6, but, top panels (a) and (b), for the whole brain volume, and bottom panels (c) and (d) considering the best 10% voxels of the left hemisphere vs. the best 10% voxels of the right hemisphere.

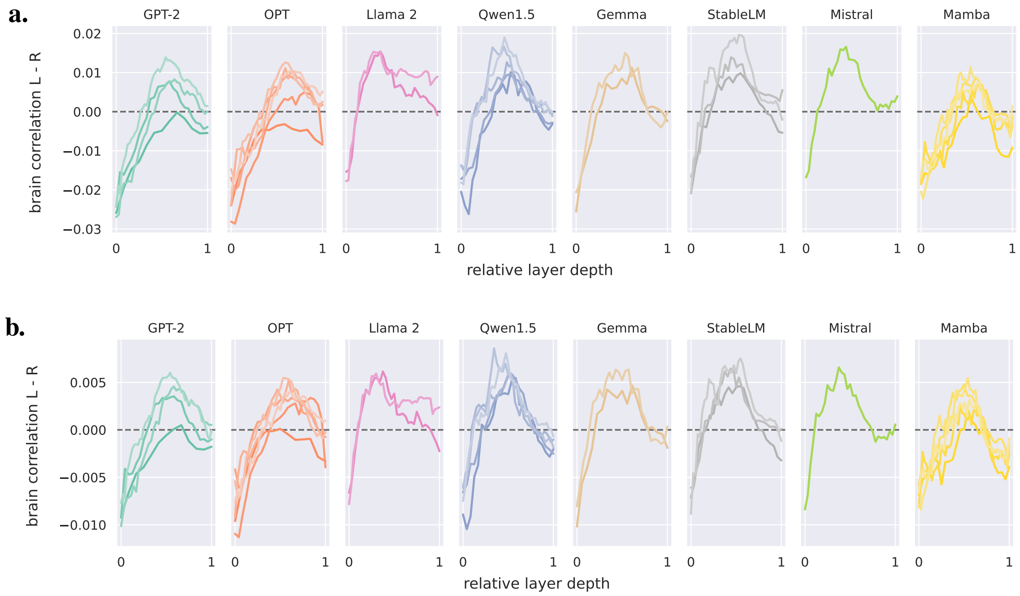

Figure B.7: **Left-right difference in brain correlation as a function of the relative layer depth, split by family**. Considering (a) the 25% most reliable voxels or (b) the whole brain volume.

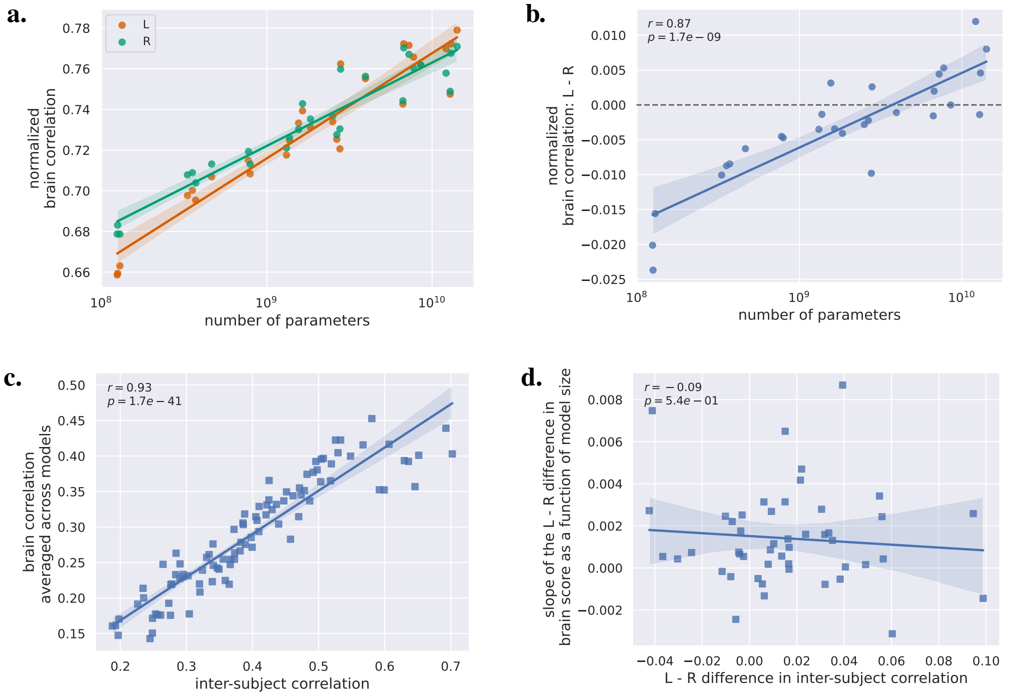

Figure B.8: **Influence of inter-subject correlations on brain scores and growth in asymmetry.** (a) and (b): Same as Fig. 6, but brain correlations are normalized by inter-subject correlations. (c) Brain correlation (average over all models) as a function of the inter-subjects correlation in each of the 48 parcels of the Harvard-Oxford atlas depicted in Fig. B.1. (d) Slope in the relationship between the L-R difference in r-score and the logarithm of the number of parameters, as a function of inter-subjects correlation. Each square corresponds to a parcel in the Harvard-Oxford atlas.

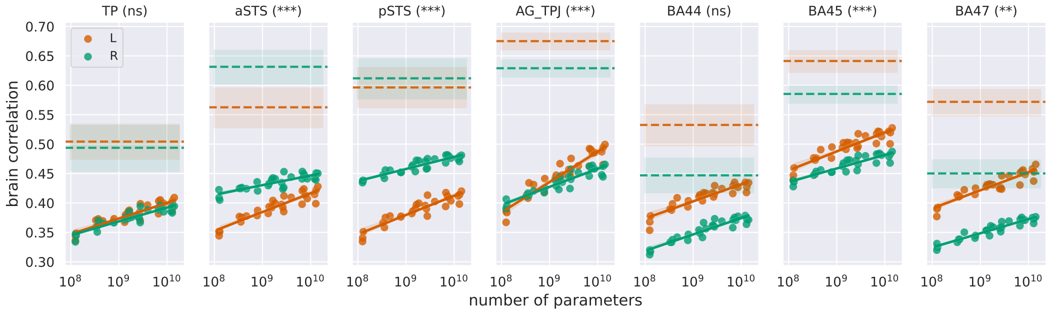

Figure B.9: **Analysis by Regions of Interest.** Brain correlation as a function of the number of parameters (in log scale), for all 28 models, for each ROI, for each hemisphere. The horizontal dashed lines represent the mean inter-subjects correlation in each corresponding ROI (along with 95% confidence interval).

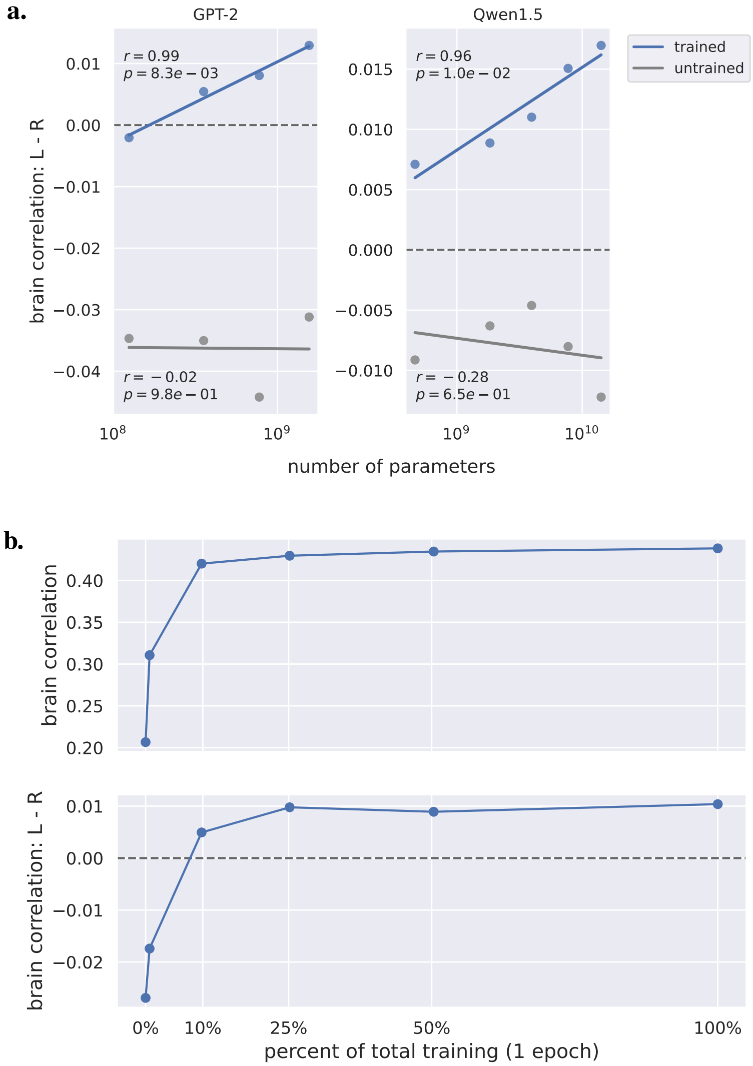

Figure B.10: **Impact of model training**. (a) Left-right difference in brain correlation as a function of the number of parameters (in log scale), for two model families (GPT-2 and Qwen1.5), before (gray dots) and after (blue dots) training. (b) Brain correlation (top) and left-right difference in brain correlation (bottom) as a function of the amount of training, for the Pythia-6.9b model. From the untrained model (0%) to the fully trained model (100% corresponds to one epoch through the 300B tokens training set). All results were computed on the 25% most reliable voxels.

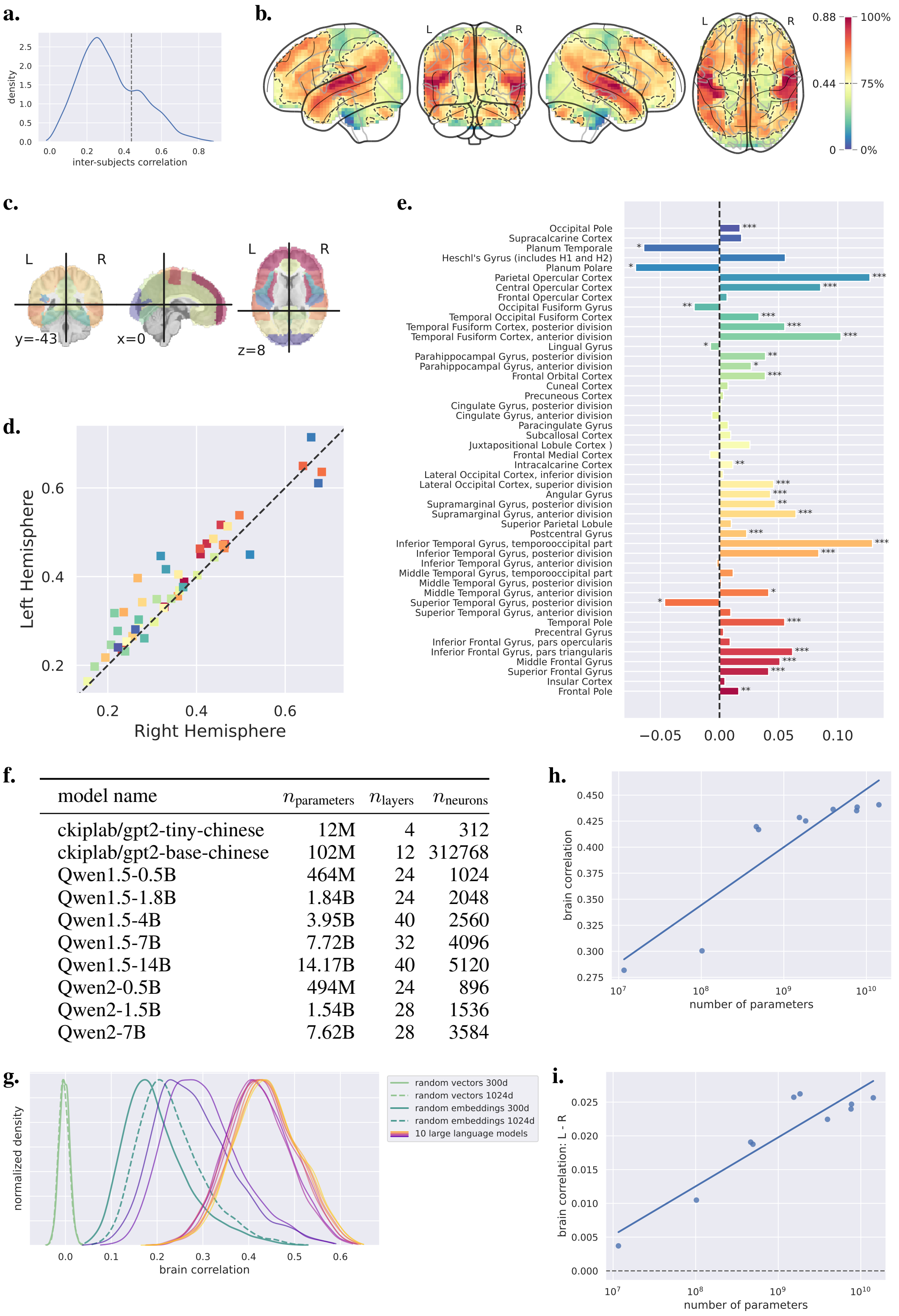

model name	$n_{\text{parameters}}$	n_{layers}	n_{neurons}
ckiplab/gpt2-tiny-chinese	12M	4	312
ckiplab/gpt2-base-chinese	102M	12	312768
Qwen1.5-0.5B	464M	24	1024
Qwen1.5-1.8B	1.84B	24	2048
Qwen1.5-4B	3.95B	40	2560
Qwen1.5-7B	7.72B	32	4096
Qwen1.5-14B	14.17B	40	5120
Qwen2-0.5B	494M	24	896
Qwen2-1.5B	1.54B	28	1536
Qwen2-7B	7.62B	28	3584

Figure B.11: **Results from Chinese participants and large language models trained on Chinese data**. Analyses performed on all 35 Chinese participants from the multilingual fMRI dataset *Le Petit Prince*. The average subject has 26050 voxels. (a,b) Same as Fig. 1 (a,b). (c,d,e) Same as Fig. B.1 (a,b,c). (f) List of all large language models used in this Chinese study (pretrained with an autoregressive objective on Chinese language data), as available on the Hugging Face hub. (g,h) Same as Fig. 2 (a, b). (i) Same as Fig. 6 (b).

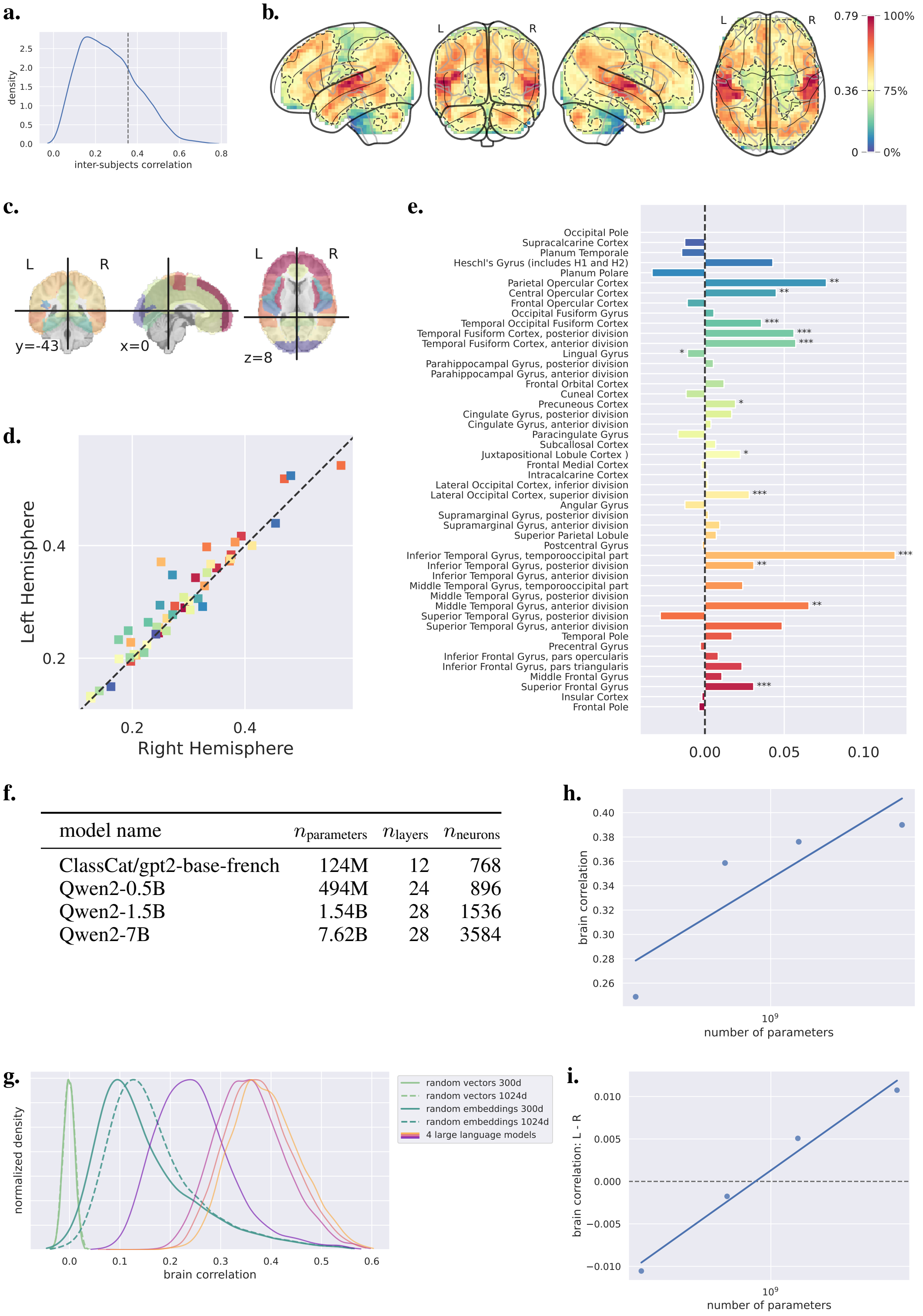

model name	$n_{\text{parameters}}$	n_{layers}	n_{neurons}
ClassCat/gpt2-base-french	124M	12	768
Qwen2-0.5B	494M	24	896
Qwen2-1.5B	1.54B	28	1536
Qwen2-7B	7.62B	28	3584

Figure B.12: **Results from French participants and large language models trained on French data**. Analyses performed on all 28 French participants from the multilingual fMRI dataset *Le Petit Prince*. The average subject has 27773 voxels. (a,b) Same as Fig. 1 (a,b). (c,d,e) Same as Fig. B.1 (a,b,c). (f) List of all large language models used in this French study (pretrained with an autoregressive objective on French language data), as available on the Hugging Face hub. (g,h) Same as Fig. 2 (a, b). (i) Same as Fig. 6 (b).

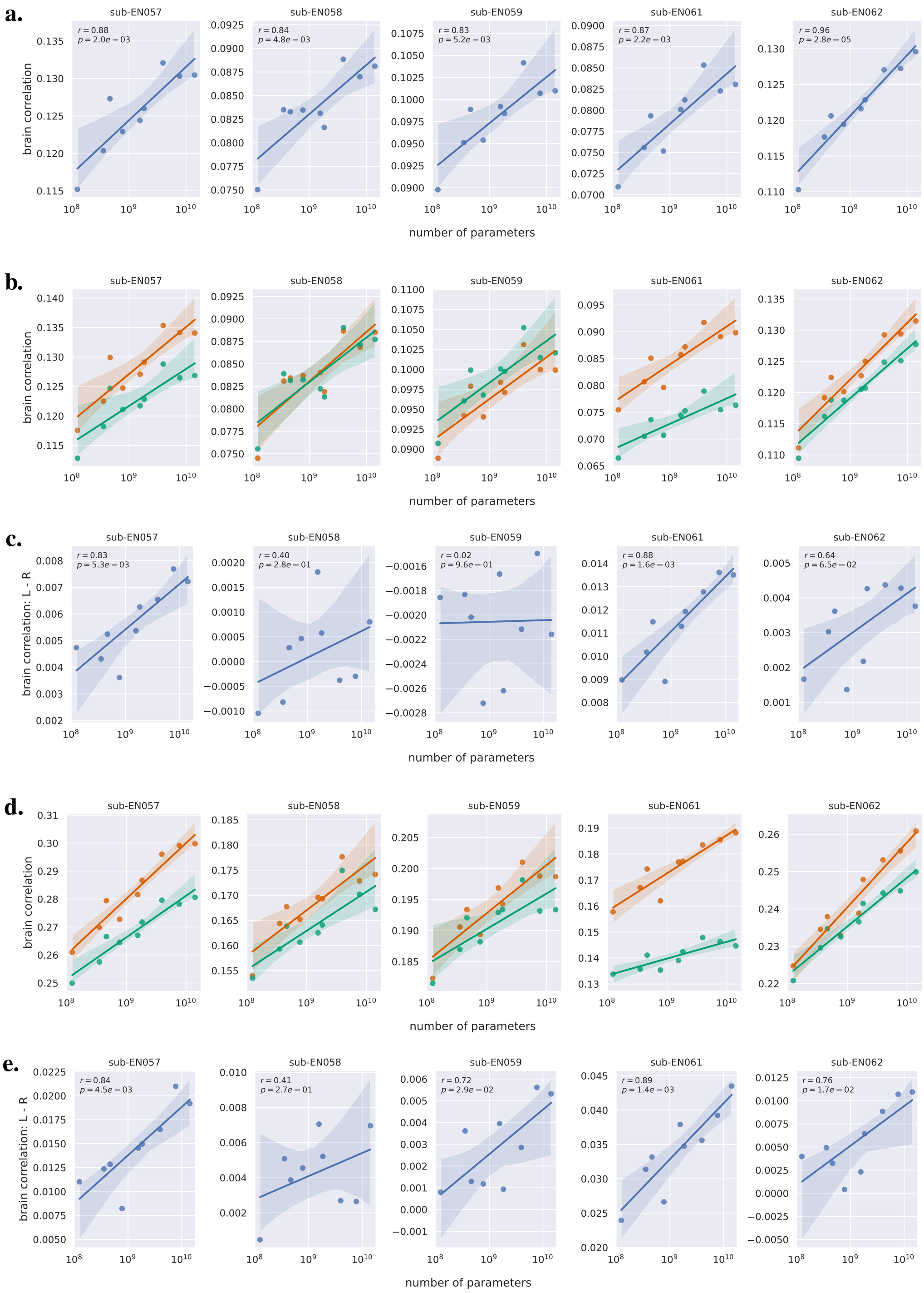

Figure B.13: **Individual analyses performed on five English participants**. Each column corresponds to one participant, `sub-EN057`, `sub-EN058`, `sub-EN059`, `sub-EN061` and `sub-EN062` respectively. Nine large language models were used: all the models from the GPT-2 and Qwen1.5 families used in the main study (see Table A.1), ranging from 124M to 14.2B parameters. (a) For each individual, brain correlation on the whole brain volume as a function of the number of parameters (in log scale). (b) Same as (a), but for the left hemisphere (red) and for the right hemisphere (green). (c) Difference between left and right hemispheric brain correlations. (d) and (e) Same as (b) and (c) but considering the best 10% voxels of the left hemisphere vs. the best 10% voxels of the right hemisphere.

NeurIPS Paper Checklist

1. **Claims**

   Question: Do the main claims made in the abstract and introduction accurately reflect the paper's contributions and scope?

   Answer: [Yes]

   Justification: The novel contribution of this work, clearly stated in both the abstract and at the end of the introduction, is the discovery of a left-right brain asymmetry in the predictive power of NLP models when their complexity increases. This is clearly supported by the experimental results presented and discussed in the paper.

   Guidelines:

   - The answer NA means that the abstract and introduction do not include the claims made in the paper.
   - The abstract and/or introduction should clearly state the claims made, including the contributions made in the paper and important assumptions and limitations. A No or NA answer to this question will not be perceived well by the reviewers.
   - The claims made should match theoretical and experimental results, and reflect how much the results can be expected to generalize to other settings.
   - It is fine to include aspirational goals as motivation as long as it is clear that these goals are not attained by the paper.

2. **Limitations**

   Question: Does the paper discuss the limitations of the work performed by the authors?

   Answer: [Yes]

   Justification: There is a dedicated subsection in the Discussion & Conclusion section, right before the References that discusses two limitations of our work (use of a group analysis rather than individual analyses, and limitation to a single language:English)

   Guidelines:

   - The answer NA means that the paper has no limitation while the answer No means that the paper has limitations, but those are not discussed in the paper.
   - The authors are encouraged to create a separate "Limitations" section in their paper.
   - The paper should point out any strong assumptions and how robust the results are to violations of these assumptions (e.g., independence assumptions, noiseless settings, model well-specification, asymptotic approximations only holding locally). The authors should reflect on how these assumptions might be violated in practice and what the implications would be.
   - The authors should reflect on the scope of the claims made, e.g., if the approach was only tested on a few datasets or with a few runs. In general, empirical results often depend on implicit assumptions, which should be articulated.
   - The authors should reflect on the factors that influence the performance of the approach. For example, a facial recognition algorithm may perform poorly when image resolution is low or images are taken in low lighting. Or a speech-to-text system might not be used reliably to provide closed captions for online lectures because it fails to handle technical jargon.
   - The authors should discuss the computational efficiency of the proposed algorithms and how they scale with dataset size.
   - If applicable, the authors should discuss possible limitations of their approach to address problems of privacy and fairness.
   - While the authors might fear that complete honesty about limitations might be used by reviewers as grounds for rejection, a worse outcome might be that reviewers discover limitations that aren't acknowledged in the paper. The authors should use their best judgment and recognize that individual actions in favor of transparency play an important role in developing norms that preserve the integrity of the community. Reviewers will be specifically instructed to not penalize honesty concerning limitations.

3. **Theory Assumptions and Proofs**

Question: For each theoretical result, does the paper provide the full set of assumptions and a complete (and correct) proof?

Answer: [NA]

Justification:

Guidelines:

- The answer NA means that the paper does not include theoretical results.
- All the theorems, formulas, and proofs in the paper should be numbered and cross-referenced.
- All assumptions should be clearly stated or referenced in the statement of any theorems.
- The proofs can either appear in the main paper or the supplemental material, but if they appear in the supplemental material, the authors are encouraged to provide a short proof sketch to provide intuition.
- Inversely, any informal proof provided in the core of the paper should be complemented by formal proofs provided in appendix or supplemental material.
- Theorems and Lemmas that the proof relies upon should be properly referenced.

4. **Experimental Result Reproducibility**

Question: Does the paper fully disclose all the information needed to reproduce the main experimental results of the paper to the extent that it affects the main claims and/or conclusions of the paper (regardless of whether the code and data are provided or not)?

Answer: [Yes]

Justification: The Methods section is devoted to exactly that. Moreover, we use a dataset publicly available, and all the code written for the project is shared with the reviewers and will be released publicly.

Guidelines:

- The answer NA means that the paper does not include experiments.
- If the paper includes experiments, a No answer to this question will not be perceived well by the reviewers: Making the paper reproducible is important, regardless of whether the code and data are provided or not.
- If the contribution is a dataset and/or model, the authors should describe the steps taken to make their results reproducible or verifiable.
- Depending on the contribution, reproducibility can be accomplished in various ways. For example, if the contribution is a novel architecture, describing the architecture fully might suffice, or if the contribution is a specific model and empirical evaluation, it may be necessary to either make it possible for others to replicate the model with the same dataset, or provide access to the model. In general. releasing code and data is often one good way to accomplish this, but reproducibility can also be provided via detailed instructions for how to replicate the results, access to a hosted model (e.g., in the case of a large language model), releasing of a model checkpoint, or other means that are appropriate to the research performed.
- While NeurIPS does not require releasing code, the conference does require all submissions to provide some reasonable avenue for reproducibility, which may depend on the nature of the contribution. For example
  (a) If the contribution is primarily a new algorithm, the paper should make it clear how to reproduce that algorithm.
  (b) If the contribution is primarily a new model architecture, the paper should describe the architecture clearly and fully.
  (c) If the contribution is a new model (e.g., a large language model), then there should either be a way to access this model for reproducing the results or a way to reproduce the model (e.g., with an open-source dataset or instructions for how to construct the dataset).
  (d) We recognize that reproducibility may be tricky in some cases, in which case authors are welcome to describe the particular way they provide for reproducibility. In the case of closed-source models, it may be that access to the model is limited in some way (e.g., to registered users), but it should be possible for other researchers to have some path to reproducing or verifying the results.

5. **Open access to data and code**

   Question: Does the paper provide open access to the data and code, with sufficient instructions to faithfully reproduce the main experimental results, as described in supplemental material?

   Answer: [Yes]

   Justification: The fMRI data comes from a publicly available dataset, and we indicate the exact version and URL of the dataset used in our study. Code will be released publicly on GitHub. In order to preserve anonymity, we share the code as a zip file with the submission.

   Guidelines:

   - The answer NA means that paper does not include experiments requiring code.
   - Please see the NeurIPS code and data submission guidelines (`https://nips.cc/public/guides/CodeSubmissionPolicy`) for more details.
   - While we encourage the release of code and data, we understand that this might not be possible, so "No" is an acceptable answer. Papers cannot be rejected simply for not including code, unless this is central to the contribution (e.g., for a new open-source benchmark).
   - The instructions should contain the exact command and environment needed to run to reproduce the results. See the NeurIPS code and data submission guidelines (`https://nips.cc/public/guides/CodeSubmissionPolicy`) for more details.
   - The authors should provide instructions on data access and preparation, including how to access the raw data, preprocessed data, intermediate data, and generated data, etc.
   - The authors should provide scripts to reproduce all experimental results for the new proposed method and baselines. If only a subset of experiments are reproducible, they should state which ones are omitted from the script and why.
   - At submission time, to preserve anonymity, the authors should release anonymized versions (if applicable).
   - Providing as much information as possible in supplemental material (appended to the paper) is recommended, but including URLs to data and code is permitted.

6. **Experimental Setting/Details**

   Question: Does the paper specify all the training and test details (e.g., data splits, hyperparameters, how they were chosen, type of optimizer, etc.) necessary to understand the results?

   Answer: [Yes]

   Justification: cf Methods section

   Guidelines:

   - The answer NA means that the paper does not include experiments.
   - The experimental setting should be presented in the core of the paper to a level of detail that is necessary to appreciate the results and make sense of them.
   - The full details can be provided either with the code, in appendix, or as supplemental material.

7. **Experiment Statistical Significance**

   Question: Does the paper report error bars suitably and correctly defined or other appropriate information about the statistical significance of the experiments?

   Answer: [Yes]

   Justification: Throughout the paper, whenever relevant, figures include error bars as well as statistical information such as correlation coefficient and p-value. We provide confidence intervals, as well as the descriptions of how these were computed, notably the factors of variability that these error bars capture. Explanations can be found in the captions of the figure, in the main text or in appendix (cf Table A.2).

   Guidelines:

   - The answer NA means that the paper does not include experiments.

- The authors should answer "Yes" if the results are accompanied by error bars, confidence intervals, or statistical significance tests, at least for the experiments that support the main claims of the paper.
- The factors of variability that the error bars are capturing should be clearly stated (for example, train/test split, initialization, random drawing of some parameter, or overall run with given experimental conditions).
- The method for calculating the error bars should be explained (closed form formula, call to a library function, bootstrap, etc.)
- The assumptions made should be given (e.g., Normally distributed errors).
- It should be clear whether the error bar is the standard deviation or the standard error of the mean.
- It is OK to report 1-sigma error bars, but one should state it. The authors should preferably report a 2-sigma error bar than state that they have a 96% CI, if the hypothesis of Normality of errors is not verified.
- For asymmetric distributions, the authors should be careful not to show in tables or figures symmetric error bars that would yield results that are out of range (e.g. negative error rates).
- If error bars are reported in tables or plots, The authors should explain in the text how they were calculated and reference the corresponding figures or tables in the text.

8. **Experiments Compute Resources**

   Question: For each experiment, does the paper provide sufficient information on the computer resources (type of compute workers, memory, time of execution) needed to reproduce the experiments?

   Answer: [Yes]

   Justification: cf section 2.3 Computer code in the Methods section

   Guidelines:

   - The answer NA means that the paper does not include experiments.
   - The paper should indicate the type of compute workers CPU or GPU, internal cluster, or cloud provider, including relevant memory and storage.
   - The paper should provide the amount of compute required for each of the individual experimental runs as well as estimate the total compute.
   - The paper should disclose whether the full research project required more compute than the experiments reported in the paper (e.g., preliminary or failed experiments that didn't make it into the paper).

9. **Code Of Ethics**

   Question: Does the research conducted in the paper conform, in every respect, with the NeurIPS Code of Ethics `https://neurips.cc/public/EthicsGuidelines`?

   Answer: [Yes]

   Justification: We reviewed the NeurIPS Code of Ethics and found that our work respects all the points.

   Guidelines:

   - The answer NA means that the authors have not reviewed the NeurIPS Code of Ethics.
   - If the authors answer No, they should explain the special circumstances that require a deviation from the Code of Ethics.
   - The authors should make sure to preserve anonymity (e.g., if there is a special consideration due to laws or regulations in their jurisdiction).

10. **Broader Impacts**

    Question: Does the paper discuss both potential positive societal impacts and negative societal impacts of the work performed?

    Answer: [No]

Justification: As we mention in the abstract, our finding reconciles results from neuroscience and machine learning, which is a positive impact for the scientific community. Yet, we cannot think of any industrial application, nor any direct risk or negative societal impact.

Guidelines:

- The answer NA means that there is no societal impact of the work performed.
- If the authors answer NA or No, they should explain why their work has no societal impact or why the paper does not address societal impact.
- Examples of negative societal impacts include potential malicious or unintended uses (e.g., disinformation, generating fake profiles, surveillance), fairness considerations (e.g., deployment of technologies that could make decisions that unfairly impact specific groups), privacy considerations, and security considerations.
- The conference expects that many papers will be foundational research and not tied to particular applications, let alone deployments. However, if there is a direct path to any negative applications, the authors should point it out. For example, it is legitimate to point out that an improvement in the quality of generative models could be used to generate deepfakes for disinformation. On the other hand, it is not needed to point out that a generic algorithm for optimizing neural networks could enable people to train models that generate Deepfakes faster.
- The authors should consider possible harms that could arise when the technology is being used as intended and functioning correctly, harms that could arise when the technology is being used as intended but gives incorrect results, and harms following from (intentional or unintentional) misuse of the technology.
- If there are negative societal impacts, the authors could also discuss possible mitigation strategies (e.g., gated release of models, providing defenses in addition to attacks, mechanisms for monitoring misuse, mechanisms to monitor how a system learns from feedback over time, improving the efficiency and accessibility of ML).

11. **Safeguards**

Question: Does the paper describe safeguards that have been put in place for responsible release of data or models that have a high risk for misuse (e.g., pretrained language models, image generators, or scraped datasets)?

Answer: [NA]

Justification:

Guidelines:

- The answer NA means that the paper poses no such risks.
- Released models that have a high risk for misuse or dual-use should be released with necessary safeguards to allow for controlled use of the model, for example by requiring that users adhere to usage guidelines or restrictions to access the model or implementing safety filters.
- Datasets that have been scraped from the Internet could pose safety risks. The authors should describe how they avoided releasing unsafe images.
- We recognize that providing effective safeguards is challenging, and many papers do not require this, but we encourage authors to take this into account and make a best faith effort.

12. **Licenses for existing assets**

Question: Are the creators or original owners of assets (e.g., code, data, models), used in the paper, properly credited and are the license and terms of use explicitly mentioned and properly respected?

Answer: [Yes]

Justification: We use a publicly available fMRI corpus, *Le Petit Prince*. We indicate the exact version that we use, as well as the URL where to find it, on openneuro.org, and cite the paper accompanying the release of this dataset. As for the code and pretrained models, we clearly list all the pretrained models and packages that we use, their versions, and we cite the relevant corresponding work for each of them. See in particular the Methods section.

Guidelines:

- The answer NA means that the paper does not use existing assets.
- The authors should cite the original paper that produced the code package or dataset.
- The authors should state which version of the asset is used and, if possible, include a URL.
- The name of the license (e.g., CC-BY 4.0) should be included for each asset.
- For scraped data from a particular source (e.g., website), the copyright and terms of service of that source should be provided.
- If assets are released, the license, copyright information, and terms of use in the package should be provided. For popular datasets, `paperswithcode.com/datasets` has curated licenses for some datasets. Their licensing guide can help determine the license of a dataset.
- For existing datasets that are re-packaged, both the original license and the license of the derived asset (if it has changed) should be provided.
- If this information is not available online, the authors are encouraged to reach out to the asset's creators.

13. **New Assets**

    Question: Are new assets introduced in the paper well documented and is the documentation provided alongside the assets?

    Answer: [Yes]

    Justification: All the code is shared along with full explanations of the procedure to exactly reproduce the results of the paper.

    Guidelines:

    - The answer NA means that the paper does not release new assets.
    - Researchers should communicate the details of the dataset/code/model as part of their submissions via structured templates. This includes details about training, license, limitations, etc.
    - The paper should discuss whether and how consent was obtained from people whose asset is used.
    - At submission time, remember to anonymize your assets (if applicable). You can either create an anonymized URL or include an anonymized zip file.

14. **Crowdsourcing and Research with Human Subjects**

    Question: For crowdsourcing experiments and research with human subjects, does the paper include the full text of instructions given to participants and screenshots, if applicable, as well as details about compensation (if any)?

    Answer: [NA]

    Justification:

    Guidelines:

    - The answer NA means that the paper does not involve crowdsourcing nor research with human subjects.
    - Including this information in the supplemental material is fine, but if the main contribution of the paper involves human subjects, then as much detail as possible should be included in the main paper.
    - According to the NeurIPS Code of Ethics, workers involved in data collection, curation, or other labor should be paid at least the minimum wage in the country of the data collector.

15. **Institutional Review Board (IRB) Approvals or Equivalent for Research with Human Subjects**

    Question: Does the paper describe potential risks incurred by study participants, whether such risks were disclosed to the subjects, and whether Institutional Review Board (IRB) approvals (or an equivalent approval/review based on the requirements of your country or institution) were obtained?

Answer: [NA]

Justification:

Guidelines:

- The answer NA means that the paper does not involve crowdsourcing nor research with human subjects.
- Depending on the country in which research is conducted, IRB approval (or equivalent) may be required for any human subjects research. If you obtained IRB approval, you should clearly state this in the paper.
- We recognize that the procedures for this may vary significantly between institutions and locations, and we expect authors to adhere to the NeurIPS Code of Ethics and the guidelines for their institution.
- For initial submissions, do not include any information that would break anonymity (if applicable), such as the institution conducting the review.